REPUBLIC OF TURKEY
ADANA ALPARSLAN TÜRKEŞ SCIENCE AND TECHNOLOGY UNIVERSITY

GRADUATE SCHOOL OF NATURAL AND APPLIED SCIENCES
DEPARTMENT OF BIOENGINEERING

CONTROLLED RELEASE OF NEUROSIN ENZYME FOR ALTERNATIVE TREATMENT OF PARKINSON'S DISEASE

EMİNE DİLA KURTUL

MASTER OF SCIENCE

ADANA 2021

REPUBLIC OF TURKEY
ADANA ALPARSLAN TÜRKEŞ SCIENCE AND TECHNOLOGY UNIVERSITY

GRADUATE SCHOOL OF NATURAL AND APPLIED SCIENCES
DEPARTMENT OF BIOENGINEERING

CONTROLLED RELEASE OF NEUROSIN ENZYME FOR ALTERNATIVE TREATMENT OF PARKINSON'S DISEASE

EMİNE DİLA KURTUL
MASTER OF SCIENCE

SUPERVISOR
ASST. PROF. DR. MERVE ÇAPKIN YURTSEVER

ADANA 2021

I hereby declare that all information in this thesis has been obtained and presented in accordance with academic rules and ethical conduct. I also declare that, as required by these rules and conduct, I have fully cited and referenced all information that is not original to this work.

[Signature]

Emine Dila KURTUL

ABSTRACT

CONTROLLED RELEASE OF NEUROSIN ENZYME FOR ALTERNATIVE TREATMENT OF PARKINSON'S DISEASE

Emine Dila KURTUL

Department of Bioengineering

Supervisor: Asst. Prof. Merve ÇAPKIN YURTSEVER

October 2021, 68 pages

Parkinson's Disease (PD) is a common neurodegenerative disorder that shows the motor and non-motor symptoms. Misfolded alpha-synuclein aggregates (Lewy bodies) are found in the brain pathology of Parkinson's patients. As a result of studies, it has been determined that these alpha-synuclein aggregates were directly related to the degrees of neurodegeneration. Although these pathological aggregates are found inside the cell, they are able to pass to healthy neurons by a prion-like mechanism. In previous studies, neurosin (Kallikrein 6, KLK6) has been shown to destroy the alpha-synuclein by cleavage at the NAC (non Amyloid-β component) region of the enzyme.

In controlled drug release systems, nanoparticles are preferred because of their nano size, allowing ease of uptake into cells. Human serum albumin (HSA), the most abundant protein in the body, is an important candidate for nanoparticle synthesis due to its easy purification, biocompatibility, biodegradability, and having many functional groups. The most common method in the synthesis of nanoparticles from HSA is the desolvation technique. In this method, generally glutaraldehyde, which has a toxic effect on cells, is used as a cross-linker.

This study, it is aimed to encapsulate neurosin, which is a therapeutic agent candidate, into HSA nanoparticles by desolvation technique. Additionally, it is aimed to reduce the toxic effect by using natural crosslinker genipin instead of glutaraldehyde in the production of HSA nanoparticles. First of all, the optimum synthesis condition for genipin-crosslinked HSA nanoparticles was determined. Zetasizer, FTIR, SEM analyzes were performed for the

characterization of the synthesized nanoparticles. Variables affecting nanoparticles production were estimated as HSA concentration, crosslinker concentration, crosslinking temperature, crosslinking time and speed of magnetic stirrer. According to the parameters examined, the optimum condition of nanoparticle synthesis was determined as 20 mg/ml HSA concentration and 0.2% w/w genipin per mg of HSA concentration. The condition of crosslinking was determined as 37°C for 2 hours at 600 rpm. Then, neurosin enzyme was loaded into HSA nanoparticles which were produced under optimum condition. Encapsulation efficiency was calculated using the ELISA kit. *In vitro* release study of neurosin loaded HSA nanoparticles was performed in PBS buffer using the dialysis membrane.

As a result of the studies, genipin cross-linked HSA nanoparticles with desired properties were produced. In the release studies of neurosin loaded nanoparticles, it was observed that neurosin was released with burst effect in the first 30 minutes. Afterward, it was observed that the drug release continues slowly according to the samples taken for 7 days. It is predicted that neurosin-loaded genipin-crosslinked HSA nanoparticles will contribute to the drug delivery systems and literature as an alternative drug system in Parkinson's disease.

Keywords: Parkinson's disease, neurosin (KLK6), nanoparticles, controlled drug release, HSA, genipin

ÖZET

PARKİNSON HASTALIĞI'NA ALTERNATİF BİR TEDAVİ İÇİN NÖROSİN ENZİMİNİN KONTROLLÜ SALIMI

Emine Dila KURTUL
Biyomühendislik Anabilim Dalı
Danışman: Dr. Öğr. Üyesi Merve ÇAPKIN YURTSEVER
İkinci Danışman: Dr. Öğr. Üyesi İsim SOYİSİM
Ekim 2021, 68 sayfa

Parkinson Hastalığı (PH), motor ve non-motor belirtilerle ortaya çıkan yaygın bir nörodejeneratif bir hastalıktır. Parkinson hastalarının beyin patolojisinde yanlış katlanmış alfa-sinüklein agregatları (Lewy cisimcikleri) görülmektedir. Çalışmalar sonucunda, bu alfa-sinüklein birikiminin nörodejenerasyon derecesi ile doğrudan ilişkili olduğu belirlenmiştir. Bu patolojik agregatlar hücre içinde bulunmakla birlikte prion benzeri bir mekanizmayla sağlıklı nöronlara da geçmektedir. Literatürde nörosin enziminin, alfa-sinüklein yapısını NAC (non Amyloid-β component) bölgesinden keserek yıkımına neden olduğunu gösteren çalışmalar bulunmaktadır.

Kontrollü ilaç salım sistemlerinde nanopartiküller, nano boyutları sayesinde hücre içine alım kolaylığı gibi avantajlarından dolayı tercih edilmektedir. Son zamanlarda, insan vücudunda en bol bulunan insan serum albumin (HSA) proteini; kolay saflaştırılabilmesi, biyouyumluluk, biyolojik olarak bozunabilirlik, toksik olmaması ve çok sayıda fonksiyonel gruba sahip olması nedeniyle nanopartikül üretiminde önemli bir adaydır. İnsan albumin proteininden nanopartikül üretiminde en sık kullanılan yöntem desolvasyon tekniğidir. Bu yöntemde çapraz bağlayıcı olarak toksik etki gösteren glutaraldehit kullanılmaktadır.

Bu çalışmada; terapötik ajan adayı olan nörosin, desolvasyon tekniği ile insan serum albumin nanopartiküllerine kapsüllenmesi hedeflenmiştir. Ayrıca, HSA nanopartikülü üretiminde glutaraldehit yerine doğal çapraz bağlayıcı olan genipin kullanılarak toksik etkinin azaltılması

hedeflenmiştir. Çalışma kapsamında ilk olarak, genipin ile çapraz bağlanmış HSA nanopartikülleri için optimum üretim koşulu belirlenmiştir. Sentezlenen nanopartiküllerin karakterizasyonu için Zetasizer, FTIR ve SEM analizleri gerçekleştirilmiştir. Nanopartikül üretimine etki eden değişkenler; HSA konsantrasyonu, çapraz bağlayıcı konsantrasyonu, çapraz bağlanma sıcaklığı, çapraz bağlanma süresi ve manyetik karıştırma hızı olarak seçilmiştir. İncelenen parametreler ışığında, nanopartikül koşulları olarak 20 mg/ml HSA konsantrasyonda, %0.2 w/w genipin HSA oranı olarak belirlenmiştir. Çapraz bağlanma koşulu ise %0.2 w/w genipin/HSA oranı ile 600 rpm'de 2 saat 37°C olarak belirlenmiştir. Böylece glutaraldehit ile 24 saat olan çapraz bağlanma süresi 2 saate düşürülmüştür. Daha sonra, optimum koşulda üretilen HSA nanopartiküllerine nörosin enzimi yüklenmiştir. Enkapsülasyon verimi ELISA kit kullanılarak hesaplanmıştır. Neurosin yüklü HSA nanoparitküllerinin *in vitro* salım çalışmaları diyaliz membran kullanarak PBS tamponunda gerçekleştirilmiştir.

Yapılan çalışmalar sonucunda istenilen özelliklerde genipin ile çapraz bağlanmış HSA nanopartikülleri üretilmiştir. Optimum koşul olarak seçilen HSA nanopartiküllerine nörosin yüklenerek salım çalışmaları gerçekleştirilmiştir. İlk 30 dakika içinde patlama etkisi ile nörosinin salındığı görülmektedir. Daha sonra 7 gün boyunca alınan örneklerle ilaç salınımının yavaş devam ettiği görülmektedir. Nörosin yüklü genipin ile çapraz bağlanmış HSA nanopartiküllerinin, ilaç taşıyıcı sistemlerinin gelişimine ve Parkinson hastalığında etkin alternatif bir ilaç olarak literatüre katkıda bulunacağı öngörülmektedir.

Anahtar Kelimeler: Parkinson hastalığı, nörosin (KLK6), nanopartikül, ilaç salımı, HSA, genipin

Dedication to my mum and my grandma who always believe in me

Words are not enough to express my love for you

ACKNOWLEDGEMENTS

Finishing this thesis through these challenging times would not have been possible without the support of some people. I would like to extend my sincere gratitude for every one of them.

First and foremost, I would like to express my deepest gratitude to my supervisor Asst. Prof. Merve Çapkın Yurtsever for her continued guidance and encouragement over these past years. Her phone was always open whenever, I ran into a trouble spot or had a question about my experiments, even late at night. I understand better how lucky I am to work with her who gave me the opportunity to improve myself in this field that I have been interested in many years. I deeply thank for her invaluable assistance; without her, finding my way would not have been possible.

I would like to thank my thesis committee members, Prof. Dr. Fazilet Aksu and Prof Dr. Mehmet Bertan Yılmaz, your ideas and feedback will intellectually contribute to my development.

I thank all my lab mates; Gözde Güldağ, Alican Cömertpay, Kübra Temiz who were always ready to help with troubles that I had in the lab. Collaboration among us that has meant every single one of you has played a support role and I thank you all for that.

I also would like to thanks to my friends; Tansu, İsmail, Arzu, Taha, Gamze, Menekşe and other friends who directly and indirectly provide me inspirations and valuable support during these stressful years.

My dear friend, T.Yasir Demirtaş, you were always there, wherever and whenever that was. Each midnight, every morning, each time I cried, and I struggled to find a way to set things right. I honestly hope our working relationships and friendships continue for many years to come. Thank you for everything.

Most importantly, none of this could have happened without my family. My mother and my grandmother, who offered their encouragement through phone calls every day. To my family, every time I felt like I couldn't go on, you all keep me motivated. I am forever grateful to all of you.

Thanks to TÜBİTAK for awarding me a National Scholarship in Priority Fields in Science-2210/C Fellowship, providing me with the financial means to complete this thesis.

This thesis was financially supported by ATU BAP Coordination Unit with project number of 20332001.

TABLE OF CONTENTS

LIST OF FIGURES

LIST OF TABLES

NOMENCLATURE

AADC	: DOPA Decarboxylase
AAV	: Adeno-associated virus vectors
BSA	: Bovine Serum Albumin
COMT	: Catechol-O-methhyl Transferase Inhibitors
DA	: Dopamine
DBS	: Deep Brain Stimulations
DDC-I	: Dopa-decarboxylase Inhibitors
DLB	: Dementia with Lewy Body
DNA	: Deoxyribonucleic Acid
ECM	: Extracellular Matrix
EE	: Encapsulation Effiency
ESCs	: Embriyonic Stem Cells
FDA	: US Food and Drug Administration
FTIR	: Fourier Transform Infrared Spectroscopy
GID	: Graft Induced Dyskinesia
GNP	: Genipin
GPi	: Globus Pallidus
HSA	: Human Serum Albumin
iPSC	: Induced Pluripotent Stem Cells
KLK-6	: Kallikrein-6
LB	: Lewy Body
L-DOPA	: Levodopa
MAO-B	: Monoamine Oxidase Type B
MSA	: Multisystem Atrophy
MWCO	: Molecular Weight Cutt Off
NaCl	: Sodium Chloride
NNI	: National Nanotechnology Initiative
NP	: Nanoparticle
PBS	: Phosphate Buffered Saline

NOMENCLATURE

PD	: Parkinson’s Disease
PdI	: Polydispersity Index
RNA	: Ribonucleic Acid
SEM	: Scanning Electron Microscope
SNpc	: Substantia Nigra Pars Compacta
STN	: Subthalamic Nucleus
TH	: Tyrosine Hydroxylase
UPW	: Ultra Pure Water
UV-VIS	: Ultraviolet-visible Spectrophotometry
VM	: Ventral Mesencephalon
Z-ave	: Z-average
Z-pot	: Z-potential
α-syn	: Alpha-synuclein

1. INTRODUCTION

1.1. Motivation

Parkinson's Disease (PD) is the second most common type of neurodegenerative disease in the world. PD initially appears in patients as a motor-symptoms like resting tremor, bradykinesia, rigidity, and postural reflex impairment. Non-motor symptoms also appear in patients over time such as anosmia, constipation, sleep disturbances, cognitive decline, anxiety, and depression. PD is caused by degeneration and irreversible loss of dopaminergic neurons which are in the substantia nigra region of the brain. Lewy bodies which are the excessive accumulation of alpha-synuclein are found in the brain pathologies of patients with PD. Several studies have identified that the accumulation of alpha-synuclein is directly associated with neurodegeneration (Feany & Bender, 2000).

Current treatment options for PD consist of dopaminergic drugs and deep brain stimulation which can be applied to the limited number of patients. However, since PD is a progressive disease, dopaminergic drugs become insufficient over time and their long-term use causes side effects. Therefore, there is a need to develop new alternative treatments to slow the progression of the disease and provide long-term benefits. One of the new approaches is that aims to reduce pathological alpha-synuclein aggregates (Stoker, Torsney, & Barker, 2018). In previous studies, neurosin has been shown to destroy the alpha-synuclein by cleavage at the NAC region of alpha-synuclein (Spencer et al., 2015). Additionally, inactive neurosin has been discovered in pathological alpha-synuclein aggregates. In the light of this information, it is suggested that a decrease in neurosin activity is associated with an increase in alpha-synuclein pathology in PD (Kasai et al., 2008).

Human serum albumin (HSA) is a useful candidate for drug delivery systems. HSA has a high ligand binding capacity and is a carrier for endogenous and exogenous compounds. High bioavailability, biodegradable properties, and easy production are the advantages of HSA (Kratz, 2008, 2014). Generally, the desolvation technique is used for albumin nanoparticle production. Glutaraldehyde, which has toxic effects on cells, is preferred as a crosslinker in the desolvation technique (Elzoghby, Samy, & Elgindy, 2012).

Genipin is a non-toxic, highly biocompatible crosslinker extracted from natural sources. Genipin also has a wide variety of pharmacological properties. These properties are anti-inflammatory, neuroprotective, neurogenic, anti-diabetic, anti-tumor, and anti-depressive (Li, Li, & Hölscher, 2016).

1.2. Aim

It is aimed to encapsulate neurosin, which is a therapeutic agent candidate, into HSA nanoparticles by desolvarion technique. Additionally, it is aimed to reduce the toxic effect by using natural crosslinker genipin instead of glutaraldehyde in the production of HSA nanoparticles. Firstly, albumin-based nanoparticles have been improved to reduce the toxic effect by using the natural crosslinker genipin instead of glutaraldehyde. After that, the production of nanoparticles containing neurosin that is capable of degrading the alpha-synuclein has been improved and its suitability for drug delivery system has been analyzed. There has been no study in the literature that aims to improve a drug delivery system through encapsulating the neurosin into nanoparticles.

1.3. Contribution

In this thesis, the method of HSA nanoparticle synthesis was optimized by using the natural crosslinker genipin instead of glutaraldehyde. A controlled release study was performed after loading the neurosin enzyme under the determined optimum conditions. The novel drug delivery system is expected to have a protective effect on neurons by reducing neuronal death. The development of drug delivery systems will lead to the development of personalized medicine with future studies in humans. It is also thought that the results obtained will lead to other projects to be written in the future since it is a research topic that has not existed in the literature.

2. LITERATURE REVIEW

2.1. Parkinson's Disease

Parkinson's Disease (PD) is the second most common type of progressive neurodegenerative disorder after Alzheimer's Disease, with an incidence of 1-2% in people over 65 years of age. The incidence of PD is thought to be double within 20 years. Motor symptoms of PD are caused by degeneration and irreversible loss of dopaminergic neurons located in substantia nigra pars compacta (SNpc) projecting to the dorsal striatum, which consist of the caudate and putamen (de Lau & Breteler, 2006; Harris et al., 2020). This depletion of dopaminergic neurons and intraneuronal proteinaceous cytoplasmic inclusions, known as Lewy Bodies are pathological hallmarks of Parkinson's Disease (Dauer & Przedborski, 2003). Lewy bodies are thought to cause loss of neurons in SNpc (Harris et al., 2020). The main constituent of Lewy pathology is the excessive accumulation of alpha-synuclein, a protein normally located in synaptic terminals of neurons (Figure 2.1) (Harris et al., 2020; Raza, Anjum, & Shakeel, 2019). Motor and non-motor symptoms appear in Parkinson's patients due to a lack of dopamine secretion. When the symptoms of PD reveals, 60% of SNpc dopaminergic neurons have already died (Dauer & Przedborski, 2003). The symptoms of PD involve resting tremor, bradykinesia, rigidity, postural and gait impairment. Non-motor symptoms also appear in patients, such as constipation, anosmia, sleep disturbances, cognitive decline, anxiety, and depression, which severely reduces the quality of the PD patients (Kalia & Lang, 2015).

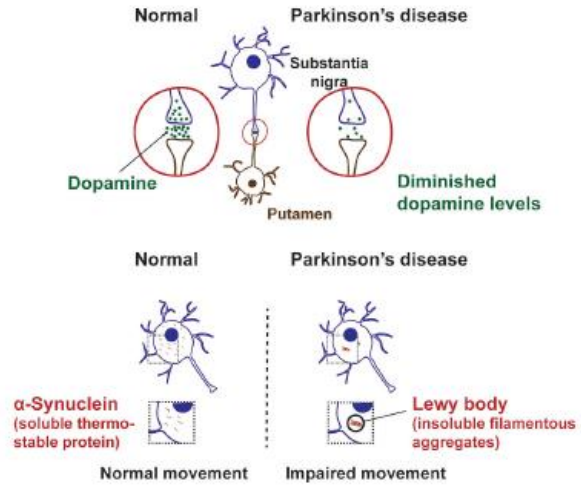

Figure 2.1. Comparison of healthy and individuals with PD, insoluble filamentous a-syn aggregates called Lewy body causes decreasing dopamine (Raza et al., 2019)

When PD was shown chronologically, nearly 100 years after being identified as shaking palsy, it was discovered that the pathological lesion of PD was in substantia nigra and that degeneration of SNpc caused motor symptoms. In 1912 and 1919, post-mortem studies conducted with the brains of PD patients revealed that there was a neuronal loss in substantia nigra and some protein aggregates in the remaining cells. These protein aggregates were entitled ‘corps de Lewy’ (Lewy body, LB) by Friederich H. Lewy. In the 1960s, it was discovered that neuronal loss in substantia nigra caused loss of DA in the basal ganglia of Parkinson's patients. It has also been shown that the use of a precursor of DA, which is capable of crossing the blood-brain barrier called L-Dopa and noradrenalin, could bring DA level to be normal. Thus, it allows the motor symptoms to alleviate. L-dopa became the first US Food and Drug Administration (FDA) approved drug used to treat Parkinson's disease (Figure 2.2) (Geibl, Henrich, & Oertel, 2019).

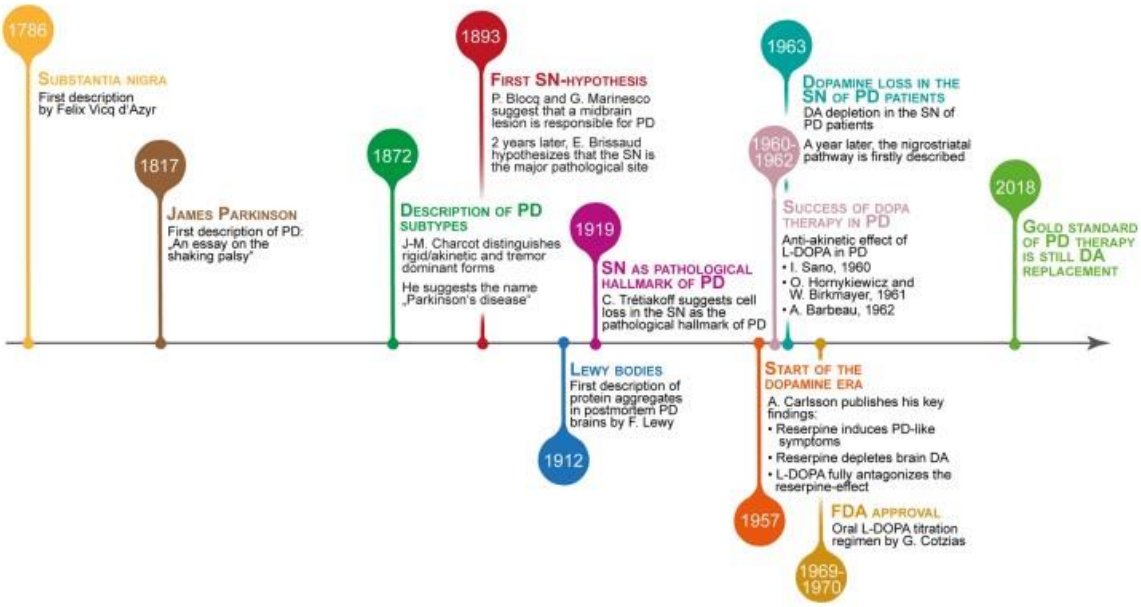

Figure 2.2. Pathology and therapy of Parkinson's disease choronologically (Geibl et al., 2019)

The etiology of Parkinson’s Disease and the relationship between LB and pathogenesis of the disease is still not fully understood. But, studies have shown that both mutations of many genetic factors and environmental factors play a role in the development of the disease (Stoker et al., 2018). Lewy pathology, which is the gold standard in the diagnosis of the disease, can be found in the spinal cord and peripheral nervous system (vagus nerve, sympathetic ganglia, cardiac plexus, enteric nervous system, salivary glands, adrenal medulla, cutaneous nerves, and

sciatic nerve) except the brain (Kalia & Lang, 2015). Braak and colleagues have suggested that Lewy pathology begins from the peripheral nervous system and spreads through the central nervous to the brain (Braak et al., 2003). Recent studies have also focused on the hypothesis that the significant role of microbiota in the pathogenesis of alpha-synucleinopathies. This hypothesis discusses that pathogenic alpha-synuclein begins at the periphery through communication between the microbiota and the immune system and then spreads to the brain (Fitzgerald, Murphy, & Martinson, 2019).

2.2. Current Treatments of PD

2.2.1. Drug Treatments for PD

The current treatment option for PD consists of pharmacologic dopaminergic drugs. Levodopa, the precursor of dopamine, is the most commonly used drug among them. Levodopa can be applied with dopa-decarboxylase inhibitors (DDC-I) to reduce the side effects of Levodopa such as, nausea. Dopamine agonist, catechol-O-methyl transferase (COMT) inhibitors, monoamine oxidase type B (MAO-B) inhibitors also can be used to renovate dopaminergic activity in the striatum (Stoker & Barker, 2020; Stoker et al., 2018). Although these medications have a good effect on motor symptoms of PD, they do not affect non-motor symptoms, including cognitive impairment, sleep disturbances, neuropsychiatric and gastrointestinal, cardiovascular, urinary, thermoregulation dysfunctions (Dong, Cui, Li, & Le, 2016). These traditional drugs also become less effective in time because of continued degeneration of dopamine cells and results in crucial adverse effects in long-term use. Side effects of these drugs observed clinically in advanced PD are thought to be due to the uncontrolled absorption of non-physiological dopamine into the striatum and its passage to areas other than the striatum (Stoker et al., 2018).

2.2.2. Deep Brain Stimulations (DBS)

DBS has also been applied as a current alternative treatment for PD. DBS is neurosurgery to place a device that sends electrical impulses to the Subthalamic nucleus (STN) and globus pallidus internus (GPi) areas of the brain (Dong et al. 2016). DBS has a significant impact on the reduction of motor symptoms of PD in severe cases where medications are ineffective; however, like dopaminergic drugs, DBS does not affect the non-motor symptoms. Additionally, the risk related to neurosurgery, some side effects like speech dysfunction and psychiatric

disturbance, and applicable for only some PD patients are adverse aspects (Poewe et al., 2017; Stoker et al., 2018).

2.3. Current Approaches for Potential PD Therapy

Medications can renovate the dopaminergic activity in the striatum. But after a while, these conventional therapies become less effective because of the progression of disease and neurons continue to die. New approaches focused on the restoration of the dopamine loss. For this purpose, studies based on the cell-based, viral gene delivery, alpha-synuclein as a therapeutic target are included in the literature (Stoker & Barker, 2020; Stoker et al., 2018).

2.3.1. Cell-Based Approaches

Different cell sources have been discovered to compensate for dopamine deficiency. The significant effect of Human fetal ventral mesencephalon (VM) tissue grafts on treating many PD symptoms has been investigated since the 1980s. The reason for ethical and logistical barriers like an insufficient supply of fetal tissue prevents this from being the primary therapy for PD. Clinical trials of stem cell-based products are currently ongoing. Center for iPS Cell Research and Application, Kyoto University, Japan conducting a clinical trial using dopaminergic progenitors that is originated from allogeneic induced pluripotent stem cells (iPSCs), NYSTEM-PD, the USA conducting a clinical trial using Embryonic Stem Cells (ESCs) are some examples of current clinical trials (Stoker & Barker, 2020).

However, some concerns regarding stem cell-based transplantation have still existed. The main problem with stem cell transplantation is that uncontrolled cell proliferation or mutations in the oncogenes of the transplanted cells may result in tumor formation (Dong et al., 2016; Poewe et al., 2017; Stoker et al., 2018).

Another drawback is which source of stem cells (autologous or allogenic) should be chosen for transplantation. The response of the immune system to grafted cells affects their viability. Transplantation of autologous grafts can be integrated itself into the injection area without any immune response. However, autologous grafts still carry genetic mutations that are associated with the development of PD (Fan, Winanto, & Ng, 2020; Fu et al., 2015).

On the other hand, the major problem after transplantation is graft-induced dyskinesia (GID). According to the report of Defer et al., dyskinesia was emerged after transplantation (Defer et al., 1996). In other studies, it has been suggested that the reason for this is that the number of cells applied is insufficient or that it should be applied with an immunosuppressive. As a result, the graft should be able to transplant to an adequate number of cells including the pure population of DA neurons (Fu et al., 2015).

2.3.2. Gene Therapy

In general, gene therapies can increase secreting of dopamine in the striatum by using viral vectors that deliver the specific gene responsible for dopamine synthesis. Tyrosine hydroxylase (TH) enzyme is required to produce a dopamine precursor known as Levodopa, and Dopa decarboxylase (AADC) provides the conversion of levodopa to dopamine. A clinical trial conducted for PD using genes that encodes these enzymes is still ongoing (Stoker & Barker, 2020). In addition, studies using Adeno-associated virus vectors (AAV) carrying genes encoding AADC, neurturin, or glutamic acid decarboxylase have been conducted in clinical trials (Christine et al., 2009; LeWitt et al., 2011; Marks et al., 2008). AAV vectors do not have the risk of mutagenesis, but the major problem with this vector is that its capacity to carry genetic material is relatively limited; that is, only one of the enzymes involved in the dopamine synthesis pathway can be loaded. On the contrary, lentiviral vectors can carry more genetic material compared to AAV vectors (Stoker et al., 2018). ProSavin® (Oxford Biomedica, United Kingdom) uses lentivirus vectors to carry genes encoding ADDC, tyrosine hydroxylase, and cyclohydrolase-1. These enzymes catalyze the synthesis of a necessary cofactor known as tetrahidrobioptrein for the synthesis of dopamine and serotonin. Advanced PD patients treated with Prosavin in clinical trials have shown improvement without side effects. However, the degree of improvements observed with ProSavin therapy was not adequate to compete (Stoker & Barker, 2020).

2.3.3. Alpha-Synuclein as a Theraupatic Target

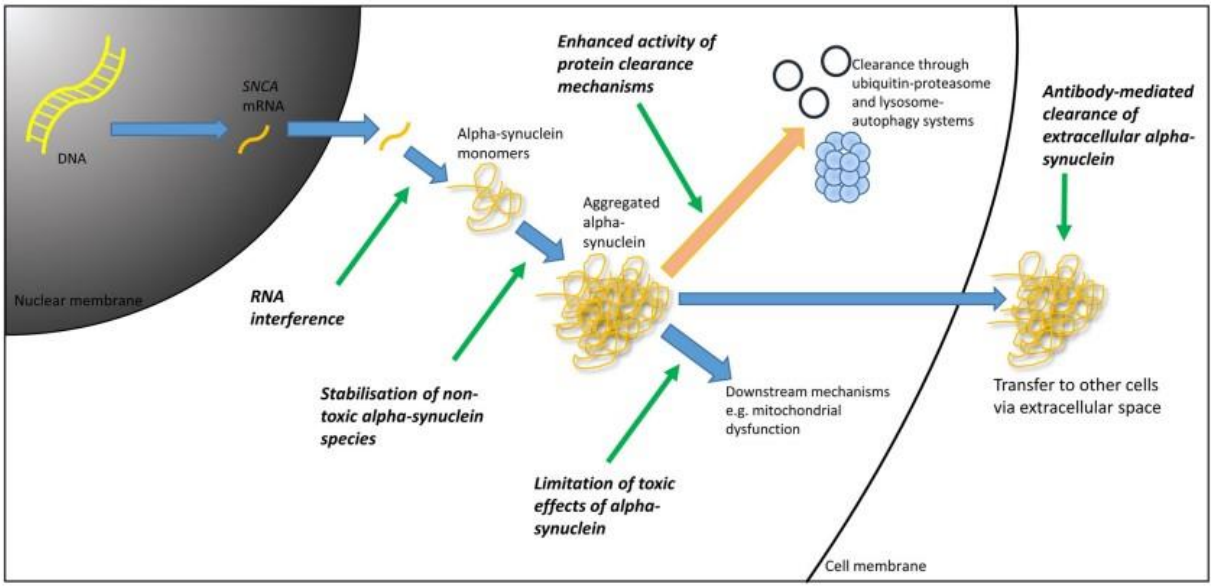

Figure 2.3. Alternative treatment approaches by targeting alpha-synuclein (Stoker et al., 2018)

Another alternative approach focuses on decreasing the levels of aggregated alpha-synuclein, which is the pathological hallmark of PD. For this purpose, some experimental methods have been investigated as to whether they would affect alpha-synuclein accumulation (Figure 2.3). Post-transcriptional silencing of the alpha-synuclein may be targeted through RNA interference technologies; that is, the exogenous introduction of synthetic ribonucleic acid (RNA) causes degradation of messenger RNA (mRNA) and suppress alpha-synuclein production. In addition to targeting the production of alpha-synuclein, enhanced the intracellular clearance mechanisms like autophagy pathways and ubiquitin-proteasome system or immune therapies to degrade extra-cellular alpha-synuclein may be helpful for PD (Stoker et al., 2018).

2.4. Alpha-Synuclein (α-syn)

Alpha-synuclein is a small protein that consists of 14 amino acids (Klein & Westenberger, 2012). Pathological aggregation of alpha-synuclein is known to be a common feature of several neurodegenerative diseases, including Parkinson's Disease (PD), dementia with Lewy bodies (DLB), and multisystem atrophy (MSA) (Gómez-Benito et al., 2020). Several different alpha-synuclein conformations have been associated with the pathogenesis of these diseases, including oligomers, protofibrils, and fibrils. Each alpha-synuclein conformation shows different properties in terms of neurotoxicity, stability, and spreading ability (Gómez-Benito et

al., 2020). Fibrillary forms of alpha-synuclein are primarily detected in Lewy bodies localized in the neuronal cell body. These intracellular structures are the distinguishing neuropathological feature of PD and DLB (Lashuel, Overk, Oueslati, & Masliah, 2013). Various evidence showing the pathogenic role of alpha-synuclein in PD:

1) Point mutations (A30P, E46K, H50Q, G51D, A53T, and A53E) and duplication or triplication of the SNCA gene cause autosomal dominant forms in PD.
2) Polymorphic variants of the SNCA gene constitute a major risk factor for the development of idiopathic PD
3) Alpha-synuclein is the main component of Lewy bodies.

To date, the etiology of PD is not yet fully known (Gómez-Benito et al., 2020). However, increasing evidence indicates that the presence of intraneuronal inclusions of alpha-synuclein affects the functional integrity of neurons and ultimately causes their death. It has been shown that alpha-synuclein aggregates can induce neuronal toxicity, leading to neuronal death by many mechanisms, including mitochondrial dysfunction, lysosomal disorder, endoplasmic reticulum stress, and synaptic dysfunction. Although the exact function of alpha-synuclein is not yet known, growing evidence supports the idea that alpha-synuclein is involved in synaptic plasticity and neurotransmitter release (Gómez-Benito et al., 2020).

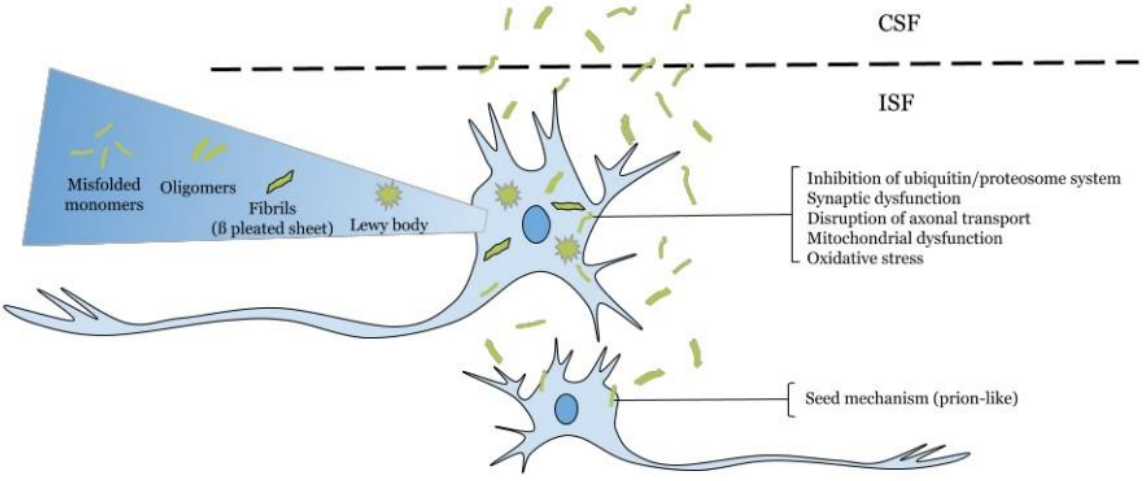

Figure 2.4. Prion-like aggretion of alpha-synuclein and effects of alpha-synuclein on neuronal cells. CSF, cerebrospinal fluid; ISF, the brain interstitial fluid (Menéndez-González, Padilla-Zambrano, Tomás-Zapico, & Fernández García, 2018).

Under normal circumstances, alpha-synuclein is assumed in the α-helix conformation, but in certain pathological situations, the protein conformation is prone to aggregation, transforming it into a ß-sheet rich structure that forms toxic species (oligomers, fibrils, and ribbons). These aggregated alpha-synuclein forms are the main component of Lewy bodies in the brains of Parkinson's patients (Vargas, Grudina, & Zurzolo, 2019). Together with two reports published in 2008, it shows that fetal mesencephalic dopaminergic neurons transplanted into the striatum for therapeutic purposes to Parkinson's patients also develop alpha-synuclein-positive Lewy bodies. As a result, it supports the hypothesis that PD is a prion-like disease by showing that alpha-synuclein can spread to healthy cells (Vargas et al., 2019) Recent studies also show that this fibril formation of alpha synuclein can spread into the nervous system by triggering a prion-like aggregation of α-syn from the neuron to the receiver neuron (Figure 2.4) (Menéndez-González et al., 2018; Terada et al., 2018).

2.5. Neurosin (KLK6, Kallikrein 6)

To prevent the proliferation of extracellular alpha-synuclein (α-syn) can be a hope to stop the progression of Parkinson's disease. Although the level of extracellular alpha synuclein is dependent on the rate of α-syn release from neural cells, the removal of these harmful proteins by using some clearance systems will be effective in preventing the progression of this disease. Examples of these clearance pathways include cell-mediated clearance proteolytic degradation, chaperone-mediated clearance, and active/passive transport out of the brain (Park & Kim, 2013).

Proteolytic degradation can be performed using several proteases, which have been previously reported to cleave and degrade the alpha synuclein. These proteases include neurosin, MMPs, and plasmin (Park & Kim, 2013).

Neurosin(kallikrein6) is a trypsin-like serine protease that is generally expressed in neurons and oligodendrocytes of the brain (Park & Kim, 2013). Neurosin consists of 244 amino acids, including 16 amino acid signal peptides and five amino acid activation peptides. It is secreted as an immature prepropeptide consisting of a signal peptide cleaved before activation through plasmin or enterokinase. In the literature, some studies show that neurosin is extracellularly active after secretion. Neurosin can destroy α-syn by cleavage in the NAC region (Park & Kim, 2013; Spencer et al., 2013).

Magklara et al. worked on this enzyme to gain information about the physiological role of neurosin. They showed that neurosin could degrade in vitro a wide variety of extracellular matrix (ECM) proteins such as fibrinogen, collagen type I – IV, and amyloid precursor protein (Magklara et al., 2003). Other studies have also shown that laminin and fibronectin (Bernett et al., 2002), proteinase-activated proteins (Ashby, Kehoe, & Love, 2010) may also be cleaved by neurosin (Magklara et al., 2003). These findings increase the possibility that neurosin may be a good option for neurogenesis and migraton of new neurons (Spencer et al., 2013). Spencer et al. have provided the evidence that α-syn in a mouse model of DLB (Dementia with Lewy bodies) can be enzymatically degraded by neurosin. They also showed that degraded α-syn had no toxic effect on neurons (Spencer et al., 2013, 2015).

Iwata et al observed the accumulation of the α-syn because of the downregulation of neurosin by siRNA. Also, they found that neurosin is present in α-syn aggregation formation called Lewy bodies (Iwata et al., 2003). In the light of this information, it is suggested that neurosin is one of the α-syn clearance enzymes and a decrease in its activity is associated with the increase of α-syn in Parkinson's patients (Kasai et al., 2008; Spencer et al., 2013; Wennström et al., 2013).

2.6. Nanoparticles in Drug Delivery

Nanoparticles are structures with sizes ranging from 1 to 100 nm, according to the description of NNI *(National Nanotechnology Initiative).* The small size of nanoparticles provides them unique physicochemical and biological features; thus, they are more readily taken up by cells than larger molecules (Wilczewska, Niemirowicz, Markiewicz, & Car, 2012). The drug delivery system can control the release of drugs, stabilize unstable molecules (proteins, peptides, or DNA) from degradation, deliver drugs to specific cells or tissue and increase bioavailability. This system also may be used to protect therapeutic drugs from enzymatic degradation (nucleases and proteases) (Singh & Lillard, 2009).

2.6.1. Characteristics of Nanoparticles as a Drug Delivery

Particle size, particle surface property, drug loading and drug release are four main factors affecting nanoparticular drug release.

2.6.1.1. Particle Size of Nanoparticles

The most significant features of nanoparticles are their size and size distribution. Toxicity, distribution in living organisms, and targeting ability of nanoparticles depend on particle size. Particle size affects drug release as well. As the size of nanoparticles is decreased, their surface area to volume ratio is increased. This indicates that the therapeutic drug is closer to the particle surface compared to larger nanoparticles, resulting in faster drug release. In addition, smaller nanoparticles are more likely to aggregate during storage, transportation, and dispersion due to the large surface area (Singh & Lillard, 2009). The role of the lymphatic system is to remove the impurities and chemicals that enter the circulation. In this case, the nanoparticle is expected not to activate the lymphatic system as much as possible. Studies have shown that particles with 200 nm and larger size tend to activate the lymphatic system (Rizvi & Saleh, 2018).

2.6.1.2. Surface Property of Nanoparticles

The surface charge properties of the nanoparticles are described by zeta potential that represents the electrical potential of particles. Zeta potential is affected by parameters such as the particle composition and the medium in which it is dispersed. Nanoparticles with a zeta potential greater than (±) 30 mV have a more stable structure in suspension, which means prevents the particles from forming aggregates (Singh & Lillard, 2009).

2.6.1.3. Drug Loading

Drug loading can be performed in two ways: incorporation of the therapeutic agents at the time of nanoparticle formation and adsorption of the therapeutic agents after synthesis of nanoparticles; this is accomplished by incubating the nanoparticles with a therapeutic agent solution. The drug loading efficiency is directly associated with the composition and molecular weight of the polymer, the drug-polymer interaction and the functional groups of the polymer (ester or carboxyl) (Singh & Lillard, 2009). In addition, the incorporation of therapeutic agents with the nanoparticles has been shown to prevent the therapeutic agent from the early degradation or inactivation after injection (Lee et al., 2014; Sebak, Mirzaei, Malhotra, Kulamarva, & Prakash, 2010).

2.6.1.4. Drug Release

The size and surface features of nanoparticles have been studied to improve bioavailability, circulation time, and stability. Controlling these features allows the drug to reach tissues or cells

that were previously inaccessible. But it would be not sensible if drug release from the nanoparticle matrix does not occur. Many factors influence drug release rate from nanoparticles, for example, pH, temperature, drug solubility, desorption of the surface-bound or adsorbed drug, drug diffusion through the nanoparticle matrix, nanoparticle matrix erosion or, degradation. Therefore, solubility, diffusion, and biodegradation of the nanoparticle matrix influence the drug release (Rizvi & Saleh, 2018; Singh & Lillard, 2009).

Drug release varies according to the type of nanoparticle used. The drug is released by the degradation of the nanoparticle matrix or by diffusion. If the drug diffusion through the nanoparticle matrix occurs faster than the degradation of the matrix, the release system is regulated by the diffusion mechanism. The weakly bound or adsorbed drug over the large surface area of the nanoparticle shows a rapid initial release profile (burst). As in many studies, when nanoparticles are placed in the release medium, a large amount of drug release before the release rate is stabilized. This is called a 'burst release'. Burst release has a negative effect on the lifetime of the system (Huang & Brazel, 2001). However, in the incorporation method, a small burst and continuous release profile are observed (Rizvi & Saleh, 2018; Singh & Lillard, 2009).

2.6.2. Human Serum Albumin (HSA) Nanoparticles

Nowadays, nanoparticles fabricated from human serum albumin (HSA) have become increasingly very popular due to their advantageous properties for drug delivery systems. Human serum albumin is a remarkably soluble protein abundant in human blood plasma and has a molecular weight of 66 500 Da and shows an average half-life of 19 days (Kratz, 2008, 2014).

The HSA protein acts as a carrier for endogenous and exogenous compounds with a high ligand binding capacity due to its hydrophobic packets (Figure 2.5) (Wang et al., 2020). Thanks to this feature, it carries out various functions in the human body. Particularly carrying fatty acids with low water solubility and hormones in the human body, making some toxins harmless and regulating pharmacokinetic properties of many drugs such as sulfonamides, penicillin, etc (Kratz, 2008, 2014). Moreover, HSA can carry the peptides/proteins by attaching these molecules to its C- and N-terminus(Wang et al., 2020). In addition to these compounds, they bind to various heavy metals to control their concentration in blood. Also, the major function

of this protein is that it regulates the colloid osmotic pressure of blood which causes water and water-soluble substances to pass from capillary vessels to tissues (Kratz, 2008, 2014).

HSA is widely used to treat various diseases including hypovolemia, shock, burn, surgical blood loss, trauma, bleeding, cardiopulmonary bypass, acute respiratory distress syndrome, hemodialysis, acute liver failure, chronic liver disease, nutritional support, resuscitation, and hypoalbuminemia. Recently, biotechnological applications of HSA involve biodegradable biomaterials, surgical adhesives and sealants, biochromatography, ligand capture and fusion proteins (Fanali et al., 2012).

This protein can remain stable in the range of 4-9 pH. It is also possible to apply heat to this protein for 10 h at 60°C. It is primarily taken from inflamed tissues and tumor cells. When it is degraded, amino acids supply nutrition to peripheral tissue (Kratz, 2008).

All in all, nanoparticles manufactured from human serum albumin for drug delivery system exhibit many advantages: having functional groups such as amino and carboxylic groups on the nanoparticle surface allows binding of albumin nanoparticles with drug targeting ligands, providing sustained release. They are biodegradable and prevents toxicity. Therefore, HSA can be an ideal drug carrier candidate.

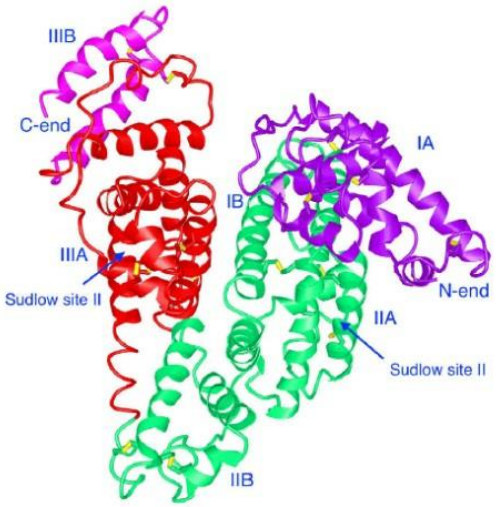

Figure 2.5. The overall structures of human serum albumin (HSA). The primary structure of has contains one N-terminus, C-terminus, three homologous domains (domain I, II and III) and subdomains (IA, IB, IIA, IIB, IIIA and IIIB) (Wang et al., 2020).

2.7. HSA Nanoparticles Preparation Methods

The role of HSA nanoparticles (HSA-NPs) loaded with a therapeutic agent is to maintain and control the release system to ensure the successful release of the therapeutic agent. Therefore, considering two different drug loading processes, it is more appropriate to immobilize the drug into the HSA-NPs matrix instead of placing it on the nanoparticle surface to improve drug stability. Furthermore, therapeutic agents, especially enzymes, are vulnerable to proteolytic degradation systems (Lee et al., 2014). For all these reasons, the best way to fabricate drug-loaded HSA-NPs seems to be encapsulation of the drug into a nanoparticle matrix.

As previously mentioned, therapeutic proteins can be protected from proteolytic degradation and also prolong release by encapsulation can be achieved. However, the environment in the polymer also affects the stability of the encapsulated protein and disrupts its integrity. This situation leads to loss of biological activity of a protein, and even worse, to release toxic degraded products. Thus, the therapeutic protein needs to be stabilized very well for successful treatment (Wolf, Wirth, Pittner, & Gabor, 2003).

Proteins can be incorporated into a matrix of HSA-NPs through some techniques. These techniques have been shown in the literature as desolvation, emulsion, coacervation, nanospray drying, self-assembly, nab-technology (Zhao, Wang, Huang, Fu, & Cheng, 2014).

Factors to be considered when choosing a method are physicochemical features and the amino acid component of the protein used as a nanoparticle, and the features of the drug to be loaded. Desolvation and emulsification are the most preferred methods in the production of protein nanoparticles (Tarhini, Greige-Gerges, & Elaissari, 2017).

Table 2.1. Active compounds encapsulated within human serum albumin (HSA) nanoparticles

Active Compund	Preparation Method	Goal	Ref.
β-galactosidase	Desolvation	Preparing 30Kc-19-HSA nanoparticles for successfull β-galactosidase delivery	(Lee et al., 2014)
Cabazitaxel	Self-assembly	Study the novel delivery system for cabazitaxel	(Zhou et al., 2016)
Paclitaxel	Nab technology	Abraxane® for treating solid tumors	(Elsadek & Kratz, 2012)
Doxorubicin	Desolvation	Study the effect of doxorubicin which is loaded into HSA nanoparticles	(Dreis et al., 2007)
Noscapine	pH-coacervation	Preparing HSA nanoparticles loaded with noscapine for potential use in breast cancer	(Sebak et al., 2010)

2.7.1. Coacervation

The coacervation technique is mainly based on the solubility of the protein in solvents according to some properties of a solvent such as pH, solvent polarity, ionic strength, or presence of electrolytes. This method decreases the solubility of the protein by causing phase separation, which is accomplished by salt addition, pH change, or non-solvent. Liquid-liquid phase separation is obtained when the salt is added to the protein solution. In this phase separation, the lower part indicates the polymer-rich phase and the upper part indicates the transparent solution, which is the result of desired nanoparticles. As a result, the desired nanoparticles are obtained (Tarhini et al., 2017). HSA nanoparticles loaded with noscapine were produced by Sebak et al. with the help of pH-coacervation technique (Sebak et al., 2010).

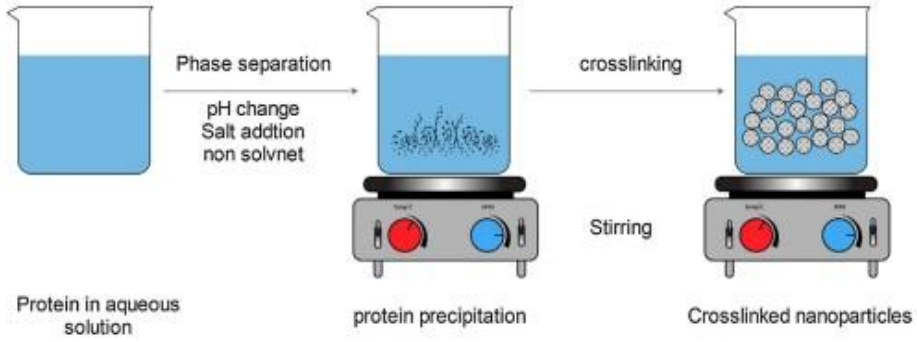

Figure 2.6. Schematic illustration of coacervation method (Tarhini et al., 2017)

2.7.2. Self-assembly

This method aims to create polymeric micelles and self-assembly of HSA by increasing the hydrophobicity of HSA. This can be achieved by way of the addition of a lipophilic drug and decreasing of primary amine groups on the protein surface (Tarhini et al., 2017).

2.7.3. Emulsification

In this method, the emulsion is formed by preparing a polymer solution in a volatile solvent. The emulsion is converted to the nanoparticle suspension by evaporation of the solvent. This method has two basic strategies, single emulsion (oil-in-water (o/ w)), double emulsions (water-in-oil-in-water (w/o/w)) (Tarhini et al., 2017). In a single emulsion (oil-in-water (o/ w), the co-solvent is selected for the water-insoluble active matter and polymer. Both are dissolved in the organic co-solvent. Nanoparticles are produced by mixing into the aqueous medium containing the surfactant (Murakami, Kobayashi, Takeuchi, & Kawashima, 2000).

In the production of nanoparticles loaded with hydrophilic molecules such as peptides or proteins, the most commonly used double emulsion (water-in-oil-in-water (w/o/w)) solvent evaporation method (supported by homogenization or ultrasonication) is used. In this method, the aqueous solution of the active substance is first dispersed in the organic phase containing the polymer. The resulting w/o emulsion is emulsified in the external aqueous phase to give the w/o/w double emulsion. The resulting w/o/w emulsion forms droplets of a polymer solution containing the active substance solution, and after removal of the solvent by diffusion or evaporation, a nanoparticle suspension containing the aqueous solution of the active substance is formed. This suspension is centrifuged to obtain nanoparticles (Murakami et al., 2000).

This method uses homogenization or ultrasonication at high speed after evaporation is carried out by continuous stirring in a magnetic stirrer at room temperature or evaporation of the solvent under low pressure. In the end, the solid nanoparticles are separated by ultracentrifugation (Tarhini et al., 2017).

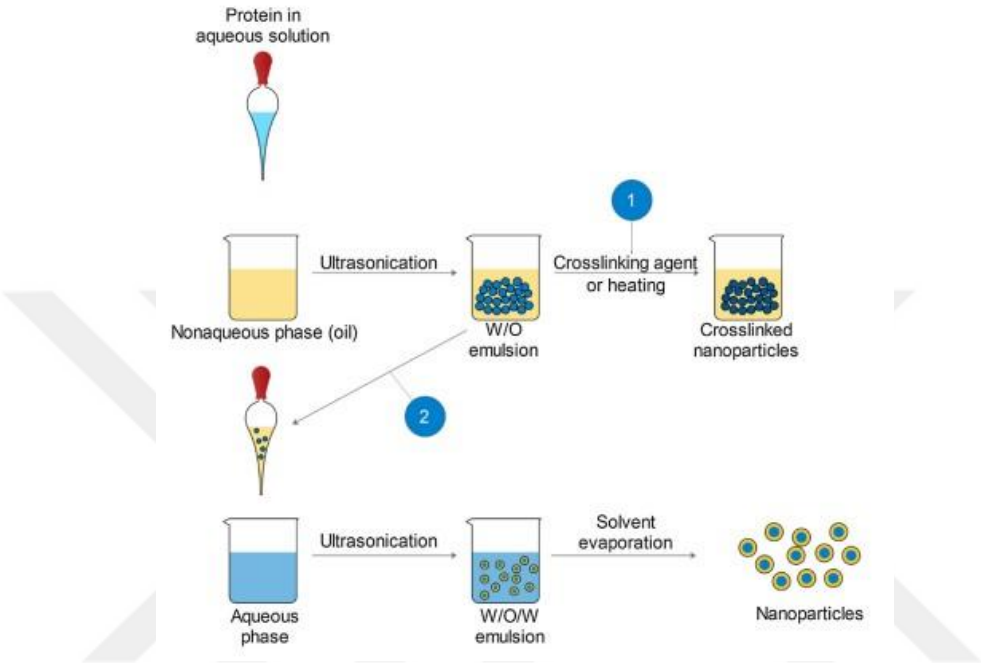

Figure 2.7. Schematic illustration of single emulsion (1) and double emulsion (2) methods (Tarhini et al., 2017)

2.7.4. Nanoparticle Albumin-Bound Technology (Nab-Technology)

Nab-technology is usually used for encapsulating lipophilic drugs into human serum albumin. In this method, the selected drug is blended with HSA in an aqueous solvent. Then, the solution is passed under high pressure through a jet to be converted to nanoparticles. Abraxane® is an FDA-approved chemotherapeutic drug that is produced by this method. In contrast to the emulsification and desolvation method, surfactants or polymeric material are not required for production in this method (Elzoghby et al., 2012).

2.7.5. Desolvation

The desolvation technique has been improved as an alternative to emulsification. Because it is a more robust and reproducible technique against possible HSA denaturation. In the emulsification process, as previously described, the organic solvent must be used. Also, oily residues and surfactants must be removed (Elzoghby et al., 2012)

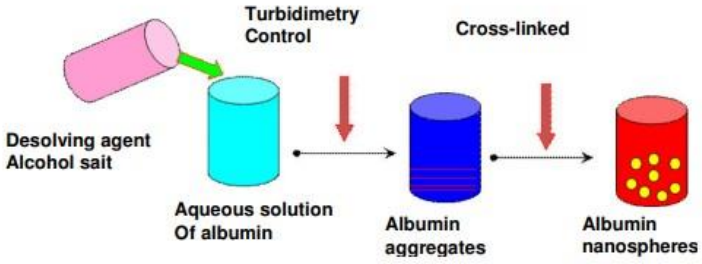

Figure 2.8. Schematic illustration of desolvation method (Rahimnejad, Mokhtarian, & Ghasemi, 2009)

HSA nanoparticles are formed by continuous ethanol addition to aqueous HSA solution under constant stirring; stirring is continued until the solution turns turbid. When ethanol is added to the solution, it is observed that its phases are separated because of reduced water solubility. After enough formation of nanoparticles, there is a need to be stabilized by using an aldehyde group of glutaraldehyde, the solid nanoparticles are obtained by the condensation reaction of coacervates. Glutaraldehyde assists the cross-linking of arginine groups in the guanidine side chains with the amino functional groups in the lysine residues, thereby allowing the albumin to solidify (Elzoghby et al., 2012). Lee et al. showed that the desolvation technique was successful in the manufacture of HSA-NPs loaded with β-galactosidase (Lee et al., 2014).

2.8. Crosslinkers

Crosslinking process is divided into two as covalent and physical. Crosslinks mean bonds in the polymer that connect one polymer chain to another. This connection is formed covalently, which is thought to be more stable between the molecules due to chemical reactions. Physical crosslinking occurs due to van der Waals forces, hydrogen bonding, or ionic interactions, etc. Crosslinkers can restrict the molecular mobility of the polymer. This restriction is required to achieve controlled release of the drug from the cross-linked polymeric drug delivery systems. Crosslinking density, polymer electrical charges, molecular mass, etc. influence drug release rates of the drug delivery system (Manickam, Sreedharan, & Elumalai, 2014).

2.8.1. Genipin

Genipin is derived from geniposide in the fruits of the plant Gardenia jasminoides Ellis, which has been used in traditional Chinese medicine to treat type 2 diabetes, headache, inflammation, and hepatic disorders and as a colorant in food industries. b-D-glucosidases is used to hydrolyze

geniposide into genipin (Figure 2.9) (Manickam et al., 2014). Experimental datas have shown that genipin has a number of significant pharmacological properties, including anti-inflammatory, neuroprotective, neurogenic, anti-diabetic, anti-tumor, and anti-depressive (Li et al., 2016).

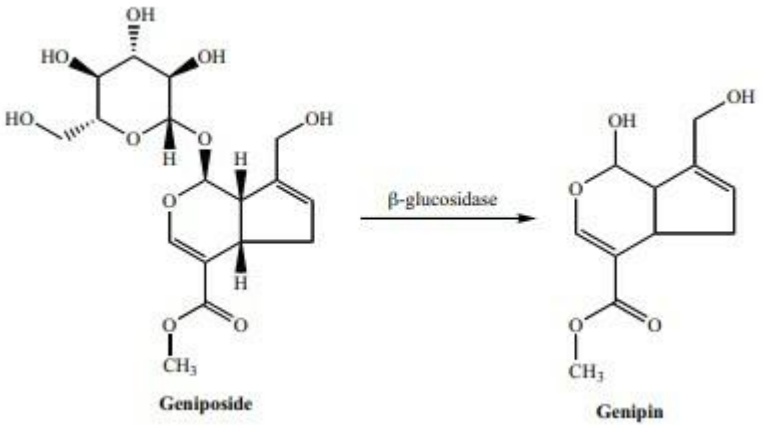

Figure 2.9. The formation of genipin by hydrolyzing b-D-glucosidase (Manickam et al., 2014)

Genipin is a natural crosslinking agent that can be used to crosslink various polymeric materials including primary amine groups, such as chitosan, collagen, gelatin, and proteins. The mechanism of genipin crosslinking is based on crosslinking of free amino groups presence in lysine, hydroxylysine, and arginine. The biocompatibility of materials crosslinked with genipin is higher than that of materials crosslinked with glutaraldehyde or any other epoxy compound (Manickam et al., 2014).

In the literature, Shahgholian et al. conducted studies on crosslinking of bovine serum albumin (BSA) with genipin instead of glutaraldehyde crosslinker by desolvation technique, which is the main method of albumin nanoparticle production. They have shown that genipin could crosslink BSA nanoparticles. In another experimental study, Luo et al. work on genipin-crosslinked human serum albumin (HSA) nanoparticles coating using a tannic acid layer. This study has shown that genipin could be able to crosslinked HSA nanoparticles, keep stable NPs, and enhance its encapsulation efficiency (Luo et al., 2020).

2.9. Drug Release Kinetics

The purpose of a controlled drug release system is to keep drug concentration in the blood or the target tissue at the desired level by controlling the drug release rate and duration. Therefore, these systems are essential for improving drug efficacy and side effects associated with dosing ('Mathematical models of drug release', 2015).

Various mathematical models have been developed to explain the release of drugs from dosage forms. Since qualitative and quantitative changes in a formulation may affect drug release and in vivo results, controlled release formulations would be necessary to predict in vivo bio-performance (Dash, Murthy, Nath, & Chowdhury, 2010).

Release datas are graphed using these mathematical models and it is determined which model is similar to the release according to the linear regression coefficient (R^2) of a graph.

2.9.1. Zero-order Kinetics

Zero order release kinetics can be expressed mathematically as;

$$\mathbf{Q_t = Q_0 + K_0 t} \qquad (2.1)$$

Q_0 = initial amount of the drug
Q_t = the amount of the drug released at the end of time t
K_0 = zero order release constant

Zero order kinetics are suitable for systems whose surface area does not change over time and which releases the drug slowly. According to this kinetics, the amount of drug released per unit time is independent of concentration and always remains constant (Singhvi & Singh, 2011).

2.9.2. First-order Kinetics

First-order kinetics are observed when the release rate is depend on the concentration and is expressed mathematically as;

$$\mathbf{\log Q_t = \log Q_0 + K_1 t/2.303} \qquad (2.2)$$

K_1 = first-order release constant

In this release kinetics, the amount of drug passing into the solution decreases over time depending on the amount of drug remaining in the matrix. Most conventional drug systems and extended-release systems accord to such release kinetics (Paarakh, Jose, Setty, & Peter, 2018).

2.9.3. Higuchi Model

In 1961, Higuchi found out possibly the most used mathematical equation. Higuchi theoretically examined the mathematical relationships that determine the release rates of the active substances from the matrix system (‘Mathematical models of drug release’, 2015). This release kinetics is expressed as;

$$\mathbf{Q_t = Q_0 + K_H t^{1/2}} \quad (2.3)$$

K_H = release constant of Higuchi

When plotting the square root graph of the amount of drug released versus time, a line whose slope is equal to the Higuchi release constant is obtained if the release is diffusion-controlled (Matrices, 1963).

2.9.4. Hixson-Crowell Model

This release kinetic is used for systems with changes in surface area and diameter during release. The release kinetics, also known as the ‘cube root law’ is defined as;

$$\mathbf{Q_0^{1/3} = Q_t^{1/3} + K_{HC} t} \quad (2.4)$$

K_{HC} = release constant of Hixson-Crowell

It gives good results in systems such as tablets where dissolution occurs parallel to the surface and the entire surface is proportionally eroded homogeneously without disturbing the geometric shape. In this model, it is accepted that the rate of drug release is determined by the dissolution rate of the drug, not to the diffusion from the matrix (Paarakh et al., 2018).

2.9.5. Korsmeyer-Peppas Model

Most of the models examining the mechanism of controlled release of the drug from polymeric systems are based on the Fick diffusion equation. However, the release mechanism may deviate from the Fick equation under experimental conditions. Therefore, this equation is used to evaluate the controlled release of polymeric systems with different geometric shapes.

$$\log\left(\frac{M_t}{M_\infty}\right) = \log k + n \log t \qquad (2.5)$$

M_t = the amount of active substance released at time t

M_∞ = the amount of active substance at the equilibrium state

k = kinetic constant expressing the structural and geometric properties of the release system

n = diffusional constant showing the release mechanism

This model is used when the release mechanism is not known or more than one release mechanism is valid. The Korsmeyer-Peppas equation is valid for the first 60% (M_t/M_∞) of the drug from the system ('Mathematical models of drug release', 2015; Paarakh et al., 2018).
The variation of the 'n' values according to release models of the active substance from polymeric matrixes with different geometries is given in Table 2.2.

Table 2.2. Values of parameter 'n' and release mechanisms for release systems with different geometric shapes ('Mathematical models of drug release', 2015)

Release mechanism model	Geometry	Release exponent (*n*)	Time in function of *n*
Fickian diffusion	Planar (thin films)	0.50	$t^{0.50}$
	Cylinders	0.45	$t^{0.45}$
	Spheres	0.43	$t^{0.43}$
Anomalous transport	Planar (thin films)	$0.50 < n < 1.0$	$t^{0.50<n<1.0}$
	Cylinders	$0.45 < n < 0.89$	$t^{0.45<n<0.89}$
	Spheres	$0.43 < n < 0.85$	$t^{0.43<n<0.85}$
Case I transport	Planar (thin films)	1.0	t([a])
	Cylinders	0.89	$t^{0.89}$
	Spheres	0.85	$t^{0.85}$
Super Case II transport	Planar (thin films)	$n > 1$	$t^{n>1}$
	Cylinders	$n > 0.89$	$t^{n>0.89}$
	Spheres	$n > 0.85$	$t^{n>0.85}$

[a] Zero-order release.

3. MATERIALS AND METHODS

3.1. Materials

3.1.1. Chemicals

Chemicals and their brands used in experimental studies are given in Table 3.1.

Table 3.1. Chemicals used in experiments

Chemical	**Company**	**Catalog No**
Albumin Fraction V Powder	Sigma-Aldrich	A16553-5G
Bovine Serum Albumin	Sigma-Aldrich	A2153-10G
Recombinant Human KLK6	Finetest	P3087
Recombinant Human KLK6	RayBiotech	230-00215-100
Human KLK6 ELISA Kit	Finetest	EH0208
%98 purity Genipin	Challenge Bioproducts	6902-77-8
Ethanol Absolute	Isolab	920.026.2500
Tube-O-DIALYZER Mini Dialysis System (50K MWCO)	G-BioSciences	786-614T
Tween-80	Isolab	9005-65-6
Phosphate Buffered Saline (PBS) 1X	Hyclone	SH30256LS

3.1.2. Devices

Precision Scale

Denver BIO.C.02 model precision scale was used to measure the weights of solid form materials used in experimental studies.

Magnetic stirrer

Isolab magnetic stirrer was used for the mixing process.

Syringe Pump

New Era Pump Systems syringe pump was used for ethanol addition in nanoparticle formation.

Shaking Incubator

IKA-Ks 4000 i control shaking incubator was used during crosslinking and *in-vitro* release studies.

pH-Meter

pH measurements of the solutions were made by Milwaukee model pH-meter.

Sonicator

ISOLAB model ultrasonic sonicator was used for homogenization and ultrasonication processes.

Ultracentrifuge

Beckman Coulter markalı Allegra 64R Centrifuge model was used for the centrifugation of nanoparticles.

Ultraviolet Visible Light Spectrophotometer (UV-VIS)

BMG-LABTECH spectrostar-Nano model Uv-vis was used to determine the amount of drug loaded on nanoparticles and released from the nanoparticles.

Zetasizer

Malvern Zetasizer-NanoZS was used for the size analysis of the nanoparticles and zeta potential measurements that show surface charge distribution

Zeta sizer device performs dimension analysis with dynamic light scattering technique (DLS), also known as photon correlation spectroscopy. It is an effective measurement method used to determine the size, size distribution and stability of particles in suspension as a result of Brownian motion and Doppler shift induced by laser light. Laser Doppler Electrophoresis (LDE) technique is used in zeta potential analysis (Sakho, Allahyari, Oluwafemi, Thomas, & Kalarikkal, 2017).

SEM (Scanning Electron Microscope)

FEI – Quanta 650 Field Emission SEM was used to examine the particle size and morphology of the nanoparticles.

Scanning Electron Microscopy (SEM) is a measurement method that analyzes the structural characteristics of the sample. High-resolution images of small areas up to 10 nm are taken even in complex samples, and three-dimensional imaging can be performed with high clarity from the desired region.

FTIR (Fourier Transform Infrared Spectroscopy)

Jasco - FT/IR-6700 was used for the characterization of nanoparticles.

The region defined as infrared is the region of the electromagnetic spectrum that falls within the range between 0.75 and 1000μm. FTIR spectroscopy measures the infrared intensity of light versus the wavenumber using the mathematical Fourier transform method. FTIR is used to analyze solid, liquid, gas and solution compounds. The method is physicochemical and is based on the principle of measuring the absorption of infrared radiation and the vibration of chemical bonds. The device provides the formation of spectral peaks thanks to changes in the vibration of the chemical bonds in the infrared region and its absorption properties.

3.2. Method

Table 3.2. Flow chart of experiment

Synthesis of HSA nanoparticles	**Stock Solution Preparation (HSA)** Crosslinking with genipin ⇩ Desolvation (addition of ethanol) **HSA-NP Synthesis** Removal of supernatant ⇩ 20.000 rpm +4°C 20 min **Ultracentrifuge** Resuspension of nanoparticles in PBS ⇩ **-20°C Storage**
Characterization of nanoparticles	**SEM Images** ⇩ **Size and Zeta-potential Analysis** ⇩ **FTIR Analysis**
In vitro Release Studies	**Neurosin-loaded HSA Nanoparticles** PBS 0.01% Tween-80 Dialysis membrane ⇩ 37°C 100 rpm Shaking incubator **In vitro Release Studies**

3.2.1. Synthesis of Empty HSA nanoparticles

In the first step, neurosin-free HSA nanoparticles were synthesized using the desolvation technique to attain optimization of nanoparticles (Figure 3.11). In principle, between 50 and 200 mg HSA were dissolved in 2.0 ml deionized water or 10 mM NaCl solution and both titrate to pH 7–10. For nanoparticle formation, 8.0 ml of desolvating agent ethanol was added (between 0.5 ml/min and 2 ml/min) as a dropwise under constant stirring (500 rpm) at room temperature. After the desolvation process, nanoparticles were cross-linked by the addition of 0.2% (w/w of HSA) genipin for at least 24h under constant stirring at 37°C in an incubator.

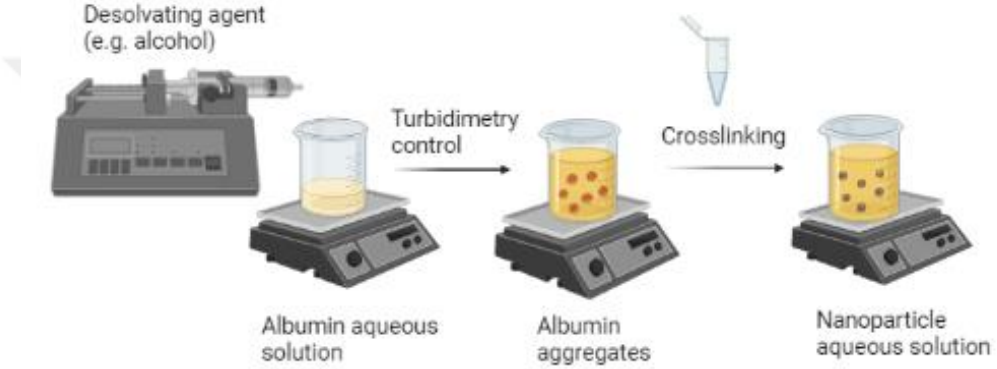

Figure 3.1. The schematic illustration of HSA nanoparticle synthesis by desolvation

Finally, empty HSA nanoparticles were purified using centrifugation (Langer et al., 2003; Lee et al., 2014). The supernatant was removed, and the particles pellet was resuspended in PBS buffer. For the elimination of undesirable substances (e.g., ethanol, genipin), the HSA nanoparticles were centrifuged and washed with ultrapure water three times (Langer et al., 2008; Lee et al., 2014).

The effect of polymer concentration, genipin cross-linker concentration, pH value, agitation speed, organic solvent adding rate and the ratio of organic solvent/polymer solution were examined for optimization studies. According to the results obtained, the most suitable nanoparticle with morphological features were selected and their chemical properties were determined in detail. The production of neurosin-loaded nanoparticle was then performed.

3.2.2. Encapsulation of Neurosin into HSA Nanoparticles

Desolvation technique was conducted to encapsulate neurosin into HSA nanoparticles.Neurosin was diluted in PBS to a final concentration of 50 μg/ml. Solubilized for 10 to 15 minutes at room temperature with gentle mixing. HSA was dissolved in purified water. The neurosin solution were added to the HSA solution under constant stirring for 15 min to obtain adsorption of neurosin into the HAS. For nanoparticle formation, 2 ml of 100% ethanol were added a dropwise under constant stirring at room temperature. Following this process, HSA nanoparticles loaded with neurosin were cross-linked by addition of 0.2% w/w genipin per mg of HSA for at least 2h under constant stirring at 37°C in an incubator. Finally, loaded HSA nanoparticles were purified using centrifugation. The supernatant was removed, and particles pellet were resuspended in UPW. For the elimination of undesirable substances (e.g., ethanol, genipin), the HSA nanoparticles were centrifuged and washed with UPW three times.

3.2.3. Size and Zeta-Potential Measurement

Zetasizer analysis was carried out to determine the size, size distribution and zeta potential of nanoparticles. For size measurement, the sample was taken from the nanoparticle suspension obtained after homogenization, and the final concentration was suspended as 0.1 mg/ml. 1.5 ml was added into the device-specific cuvette and the measurement was made by the DLS method.

3.2.4. SEM Analysis

The morphologies of the nanoparticles as examined by SEM. Their morphology was observed through SEM analysis. One droplet of diluted suspension was deposited onto a patch of silicon wafer and dried at room temperature. Then the sample was sputter-coated with gold and then investigated by SEM.

3.2.5. FTIR Analysis

The chemical structure of neurosin-loaded and neurosin-free nanoparticles was examined by Fourier transform infrared spectrophotometry (FTIR). FTIR was used to analyze the chemical composition of nanoparticles, the spectral data within the band range of 4000 to 400 cm^{-1} was recorded.

3.2.6. *In vitro* Release Studies

To investigate the release feature of neurosin-loaded HSA nanoparticles, *in vitro* release studies were performed by dialysis method in phosphate-buffered saline (PBS) containing 0.01% (v/v) Tween-80. Resuspended nanoparticles with PBS were placed into a dialysis membrane (MWCO =50 kDa) and then immersed into 5 ml PBS. The release condition was stirred at a speed of 100 rpm, 37˚C for 7 days. 250 µl of the sample was taken to estimate by ELISA-kit. This analysis was taken place at specific time intervals (15, 30, 60, 120, 720, 1440 min) and immediately replacement with an equal volume (250 µl) of fresh PBS. Absorbance reading of samples was performed at 450 nm using UV-VIS spectroscopy. Releasing of the neurosin concentration was determined by substituting the absorbance values in the equation of the calibration curve. Release values were calculated cumulatively using the time-dependent amount calculation equation in 3.1.

$$M_t = C_t \times V + \sum C_{t-1} \, x \, V_s \qquad (3.1)$$

Mt, amount of neurosin at t time(ng)
Ct, neurosin concentration at time t (ng/ml)
V is the colume of the release medium (ml)
Vs, volume of release medium taken for the measurement at certain time (ml)

The data obtained from *in vitro* release studies was adapted to various release kinetics models including zero order, first order, Higuchi, Hixson-Crowell and Korsmeyer Peppas. The linear regression coefficients (R2) of the obtained graphs was examined and the kinetic model of the release behavior will be determined.

3.2.7. ELISA Kit Measurement

Human KLK6 ELISA kit was used for quantitative detection of KLK6. The principle of this assay is based on sandwich enzyme-linked immune-sorbent assay technology. 96-well plate was pre-coated with the capture antibody. Biotin-conjugated antibodies are utilized as detection antibodies. Samples and biotin conjugated antibodies are added to the wells, and washed with wash buffer to remove unbound conjugates. After that, HRP-Streptavidin is added to wells, and washed with wash buffer. The HRP enzymatic process is seen using TMB substrates. TMB is catalyzed by HRP, resulting in a blue product that became yellow after being exposed to an

acidic stop solution. Yellow density is directly related to the amount of sample in the plate. Finally, concentration of sample can be calculated by reading the O.D.absorbance 450 nm.

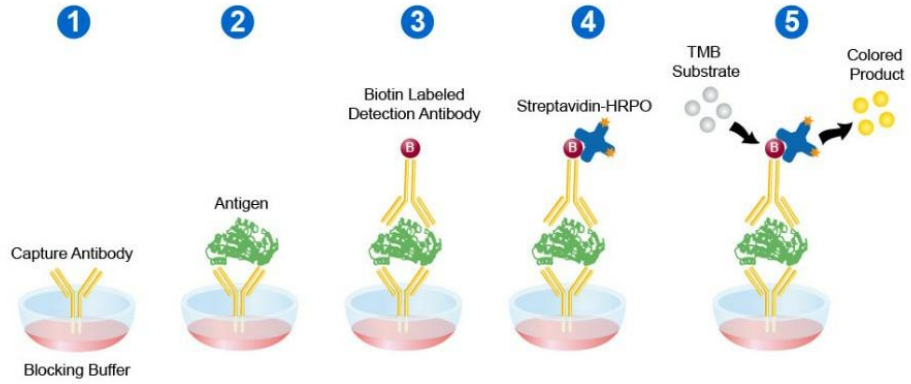

Figure 3.2. Summary of ELISA

3.2.8. Calibration Curve of Neurosin

To create the calibration curve, 20 ng of neurosin standard in the ELISA kit was dissolved with sample dilution buffer and a stock solution with a concentration of 20 ng/ml was prepared. Samples were prepared by gradually diluting the stock solution at the concentrations given in Table 3.3. After applying the Elisa assay procedure to each sample, absorbance values were measured at 450 nm using UV-Vis spectroscopy and the concentration-absorbance calibration curve was created.

Table 3.3. Neurosin concentration – absorbance values

Concentration (ng/ml)	**Absorbance (450 nm)**
20	1,9481
10	1,0236
5	0,5358
2.5	0,2549
1.25	0,1238
0.625	0,0577
0.312	0,0406
0	0

3.2.9. Encapsulation Efficiency

The supernatant, which was removed during the centrifugation step of synthesized nanoparticles, was collected in the tube and used in the analysis of free neurosin concentration. After applying the Elisa procedure, the absorbance values were found using UV-VIS spectroscopy at 340 nm. The free neurosin concentration was determined for the nanoparticle system by replacing the absorbance value read in the calibration curve equation, and encapsulation efficiency was calculated by substituting in equation 3.2.2

$$\text{EE (\%)} = \frac{Total\ Neurosin\ amount\ (ng) - Free\ Neurosin\ amount\ (ng)}{Total\ Neurosin\ amount\ (ng)}\ x\ 100 \qquad (3.2)$$

Table 3.4. Parameters in experiments

Exp.No.	Protein (g)	Neurosin (µg)	Solvent	pH	Ethanol and speed pump	Total Volume (ml)	Speed (rpm)	Crosslink conditions	Centrifuge	Washing Conditions
1	0.25 HSA	-	2.5 ml	8	7.2 (1 ml/min)	9	500	2.2% gnp, 37°C, 3h, 500 rpm	9000 rpm, 25°C, 30 min	upw
2	0.27 HSA	-	2.7 ml	8	8 (1 ml/min)	10	500	-	-	-
3	0.135 BSA	-	2.7 ml	8	8 (1 ml/min)	10	500	2.2% gnp, 25°C, 20h, 500 rpm	-	-
4	0.135 BSA	-	2.7 ml	8	8 (1 ml/min)	10	500	2.2% gnp, 37°C, 2h, 500 rpm	9000 rpm, 25°C, 30 min	-
5	0.135 BSA	-	2.7 ml	8	8 (1 ml/min)	10	500	2.2% gnp, 37°C, 2h, 500 rpm	20.000 rpm, 4°C, 15 min	Ethanol and upw
6	0.135 HSA	-	2.7 ml	8	8 (1 ml/min)	10	600	2.2% gnp, 37°C, 2h, 600 rpm	20.000 rpm, 4°C, 15 min	upw
7	0.1 HSA	-	2 ml	7	8 (1 ml/min)	10	600	2.2% gnp, 37°C, 2h, 3h,4h, 5h, 6h, 600 rpm	20.000 rpm, 4°C, 15 min	upw
8	0.01 HSA	-	500 µl	7	2 (1ml/min)	2.5	600	0.2%,2.2% gnp, 37°C, 2h, 3h, 4h, 600 rpm	20.000 rpm, 4°C, 15 min	upw
9	0.01 HSA	10	500 µl	7	2 (1ml/min)	2.5	600	0.2% gnp, 37°C, 2h, 600 rpm	23.000 rpm, 4°C, 15 min	%40 ethanol
10	0.01 HSA	10	500 µl	7	2 (1ml/min)	2.5	600	0.2% gnp, 37°C, 2h, 600 rpm	23.000 rpm, 4°C, 15 min	%40 ethanol
11	0.001 HSA	10	500 µl	7	2 (1ml/min)	2.5	600	0.2% gnp, 37°C, 2h, 600 rpm	23.000 rpm, 4°C, 15 min	%40 ethanol

4. RESULTS AND DISCUSSIONS

4.1. Optimization of HSA Nanoparticles

Experiments were conducted to estimate optimum condition for genipin crosslinked HSA nanoparticles before drug loading.

4.1.1. Protein Concentration

Exp 1, 2, 3 were conducted to estimate exact protein concentration. First of all, Langer's study, which is known as a general procedure of synthesis of HSA nanoparticles by desolvation in the literature, was used as a reference (Langer et al., 2003).

In the first experiment, 250 mg HSA was dissolved in 2.5 ml ultrapure water to be a 100 mg/ml HSA solution. After pH adjustment, it was passed through a 0.22 μm filter to remove impurities. After the filtration process, 1.8 ml of HSA solution remained. According to the general procedure, it was considered to add 8 ml (1ml/min) ethanol to 2 ml HSA solution. According to this ratio, 7.2 ml (1 ml/min) of ethanol were added to the 1.8 ml HSA solution with a syringe pump in a magnetic stirrer set at 500 rpm. When turbidity was obtained, slight coagulation was also observed on the side surface of the beaker. For the crosslinking, 2.2% (w/w of HSA) genipin was added to the HSA solution at 500 rpm and observed for 2 hours in the incubator set at 37°C. After half an hour, coagulation started to be seen in the beaker. It was sonicated and put back in the incubator. At the end of 3 hours, coagulation started to be observed more. The clumping is seen in Figure 4.1. confirmed the coagulation.

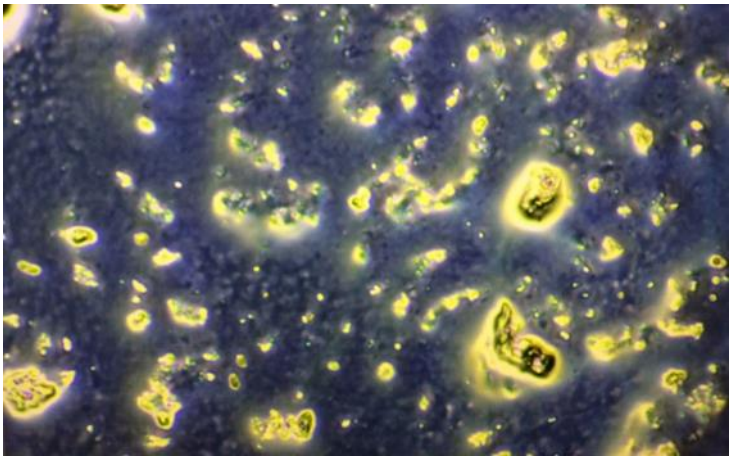

Figure 4.1. Exp 1, Microscopic image after crosslinking with genipin (32x magnification)

In the second experiment, since some of the HSA solution remained in the filter during filtration, the initial dissolution process was adjusted to 2.7 ml without changing the HSA concentration. 0.27 g HSA was dissolved in 2.7 ml ultrapure water. After pH adjustment and being filtered through a 0.22 μm filter, 8 ml of ethanol at 1 ml/min was added to 2 ml of HSA solution by using a syringe pump. Coagulation was observed in 100 mg/ml HSA solution after ethanol addition. Considering that 100 mg/ml HSA concentration was high, the next study started the 50 mg/ml HSA trial (Figure 4.2).

Figure 4.2. Exp 2, 100 mg/ml HSA solution precipitated after ethanol addition

In the 3rd experiment, 50 mg/ml BSA was used. 0.135 g BSA was dissolved in 2.7 ml ultrapure water. After pH adjustment and filtering, 8 ml of ethanol was added to 2 ml BSA by using a syringe pump under 500 rpm mixing. It was observed that homogeneous nanoparticles were obtained by microscope after ethanol addition (Figure 4.3). 50 mg/ml BSA concentration inhibited coagulation. Further studies were carried out with 50 mg/ml BSA.

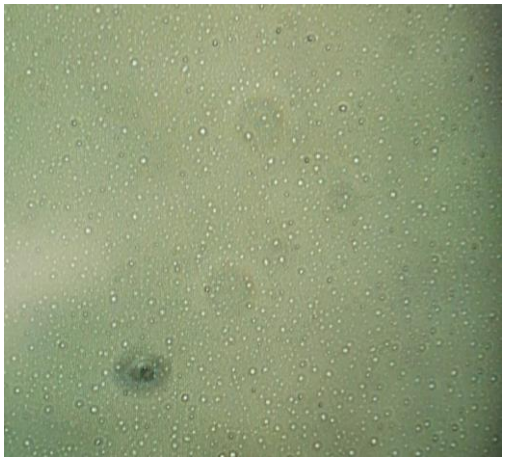

Figure 4.3. Exp 3, Nanoparticles formed in 50 mg/ml BSA solution after ethanol addition (32x magnification)

In the study of Langer et al., they reported that the minimum nanoparticle size with 155 nm was achieved by using 50 mg/ml HSA and the change in between 50 mg/ml and 100 mg/ml HSA concentration had a slight effect on nanoparticle size (Langer et al., 2003). On the other hand, Galisteo-Gonzalez and Molina-Bolivar investigated that BSA nanoparticles with 100-120 nm were synthesized in the presence of BSA concentrations between 40 mg/ml and 60 mg/ml. Therefore, the result of previous studies reveal that the concentration could be in the range of 50-60 mg/ml to synthesize albumin-based nanoparticles (Galisteo-gonzález & Molina-bolívar, 2014).

In the study of Radwan et al. performed nanoparticle production from BSA, they compared 100 mg/ml BSA concentration with lower concentrations. It was stated that the concentration of 100 mg/ml BSA was smaller and prone to aggregation because the PdI was 0.66. They determined the optimum condition as 50 mg/ml. This is also consistent with our study (Radwan, El-kamel, Burgalassi, Zucchetti, & El-moslemany, 2021).

4.1.2. Crosslinking Temperature

In a study conducted by Shahgolian et al., they used genipin instead of glutaraldehyde to produce BSA nanoparticles. Genipin solution (0.1, 0.2, 0.3% w/w of BSA) is used to crosslinked BSA nanoparticles for 24h at 25°C. In experiment 3, to improve the cross-linking method, the experiment was continued by adding genipin under room conditions. 2.2% (w/w of HSA) genipin was added and left on a 500 rpm magnetic stirrer at 25°C for 24 hours.

Coagulation was seen in the beaker after 2 hours. At the end of 20 hours, the sample collapsed (Figure 4.4).

Figure 4.4. Exp 3, Genipin crosslinked HSA nanoparticles 25°C for 24 hours

Genipin activity can be changed by temperature. Genipin was more effective and faster at 37°C (Bi et al., 2011). Therefore, experiment 4 was carried out in an incubator set at 37°C. 2.2% (w/w of HSA) genipin was added to 50 mg/ml BSA and observed for 2 hours in an incubator set at 500 rpm and 37°C. To prevent coagulation, the sample was held in a sonicator for 30 seconds every half hour. At the end of 2 hours, the sample was precipitated in a centrifuge device set at 9000 rpm 25°C for 1 hour. During the washes, the precipitated nanoparticles could not be suspended (Figure 4.5). In addition, nanoparticles could not be completely precipitated in the centrifuge device. In the next experiment, it has been started to work at high rpm for washing processes.

Figure 4.5. Exp 4, Image of nanoparticles sonicated for 45 min during washes

4.1.3. Washing Conditions

In the 5th experiment, genipin activity was thought to continue during centrifugation because it was difficult to suspend the nanoparticles during washing. Therefore, the ultracentrifuge temperature was set to 4°C. Nanoparticles were centrifugated at 20,000 rpm 4°C 15 min. Washes were done in 3 repetitions. In addition, washing was tried with an 80% (v/v) ethanol solution to remove the excess genipin more quickly. 5 ml of 10 ml nanoparticle solution was first diluted with 1:1 80% (v/v) ethanol and washing continued with 80% (v/v) ethanol. And the other 5 ml was diluted with 1:1 ultrapure water, washing was continued with ultrapure water. The suspension could not be done in a sonicator after adding 80% (v/v) ethanol. Because the nanoparticles tend to precipitate on their own because of ethanol (Figure 4.6.b) Washing with ethanol caused the nanoparticles to collapse more quickly (Figure 4.6). It has been decided that washing with ultrapure water is more efficient.

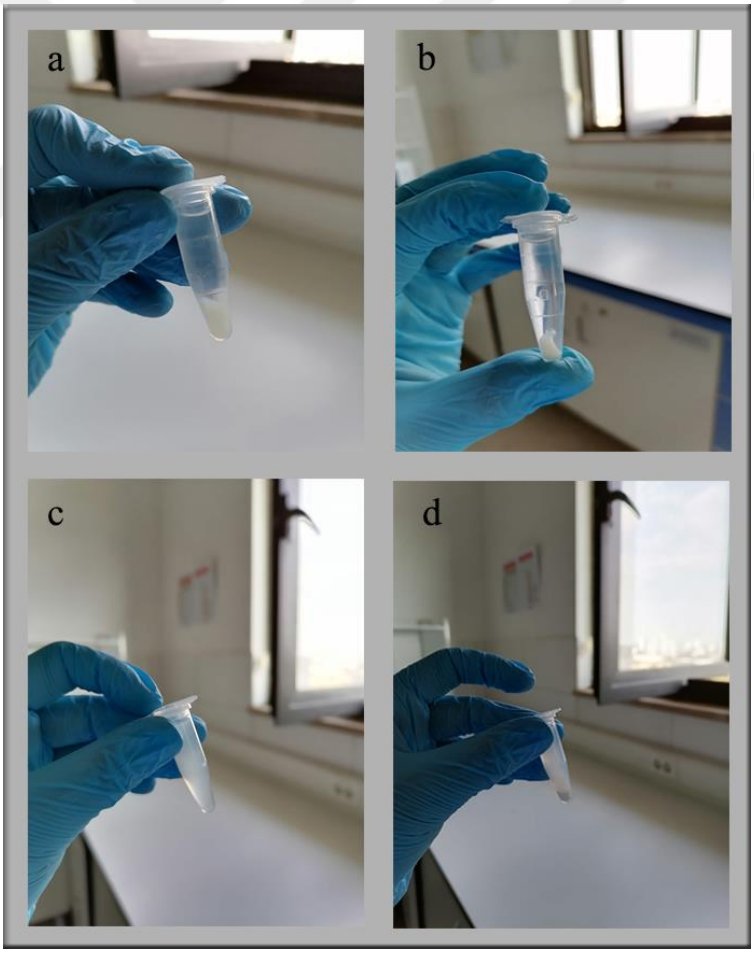

Figure 4.6. Exp 5, After centrifugation a) Nanoparticles centrifugated with ultrapure water b) Nanoparticles centrifugated with ethanol c) Suspended nanoparticles washed with ultrapure water d) Suspended nanoparticles washed with ethanol

4.1.4. Speed

In the 6th experiment, it was studied with 50 mg/ml HSA at 600 rpm mixing speed. Comparison of 500 rpm, 600 rpm, 1000 rpm mixing speeds was done. It has been observed that nanoparticle production is not efficient due to the high foaming in the HSA solution at 1000 rpm. It was observed that nanoparticles were synthesized homogeneously at 500 and 600 rpm speeds after ethanol addition. However, less coagulation was observed in the sample at 600 rpm during crosslinking.

In previous studies, HSA nanoparticle production was carried out at different mixing speeds. In studies where synthesis production was carried out at 500 and 1000 rpm, nanoparticle size was observed in the range of 100-300 nm (Langer et al., 2003; Lee et al., 2014). In an investigation by Nouri and Rafati, they observed that among the nanoparticles prepared at 200, 400, 600, 750 speeds, the most uniform HSA nanoparticles with a minimum PdI which is 0.016 at 600 rpm speed (Nouri & Rafati, 2017).

4.1.5. pH

Studies in the literature showing that crosslinking activity of genipin depends on the changing of pH. Mi et al. have shown that crosslinking of chitosan with genipin is more efficient under neutral conditions (Mi et al., 2005). Therefore, experiment 7 was continued under neutral conditions without pH adjustment.

4.1.6. Crosslinking Time

In experiment 7, to make sure about the crosslinking time, pre-wash and post-wash images of nanoparticles were taken at 2, 3, 4, 5, and 6 hours after the addition of 2.2% w/w genipin at 37°C.

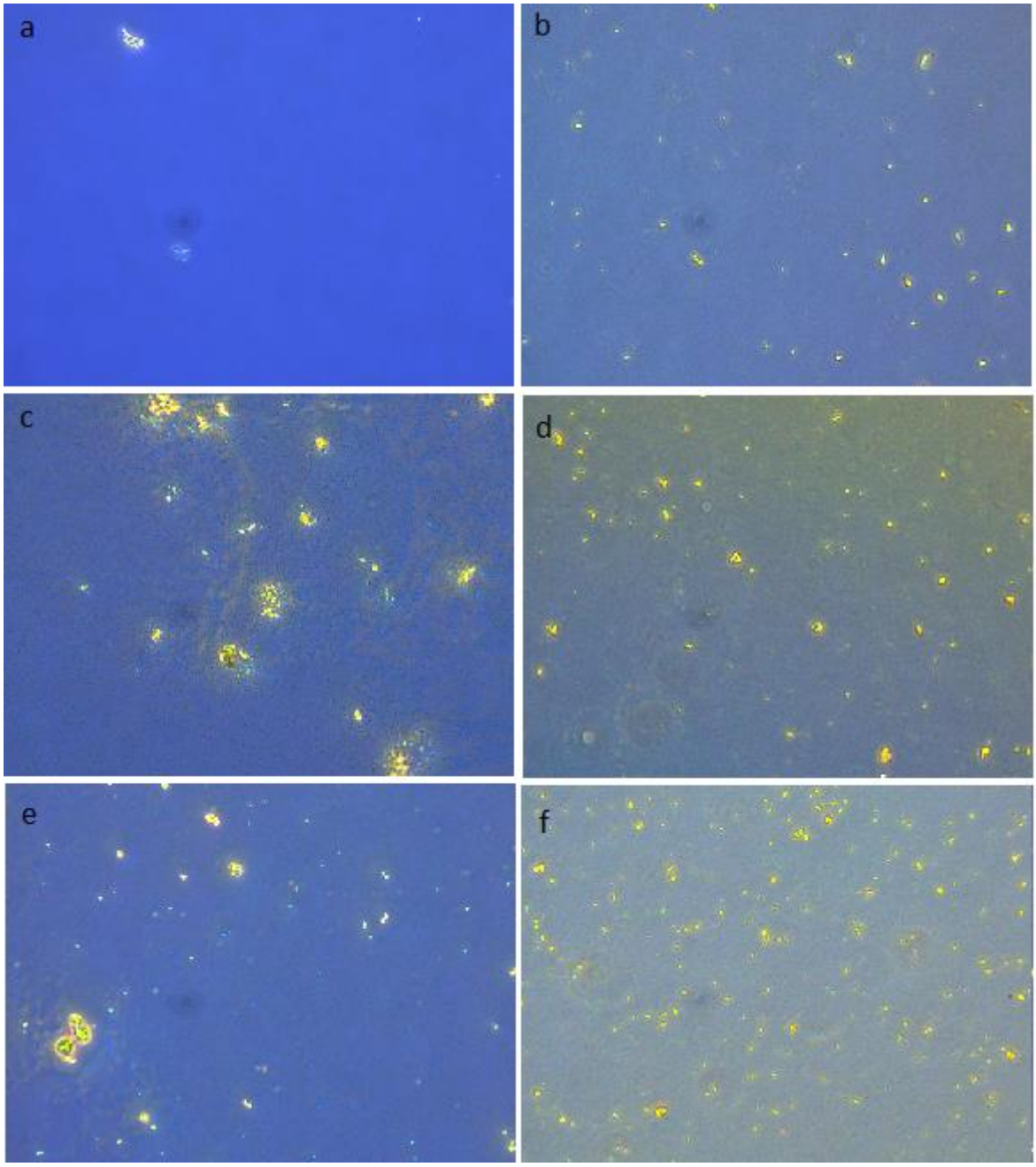

Figure 4.7. Exp 7, a)Image of nanoparticles crosslinked with 2 hours b)Image after washing process c)Image of nanoparticles crosslinked for 3 hours d)Image after washing process e)Image nanoparticles crosslinked for 4 hours f)Image after washings (32x magnification)

Microscopic images of nanoparticles crosslinked for 3 and 4 hours showed aggregate structure extremely (Figure 4.7. c, d, e, f). During the washing process, it was difficult to homogenize crosslinking nanoparticles for 3, 4 and 5 hours while suspending them. It was carried out by applying mechanical force with a pipette tip. It was observed that as the cross-linking time increased, the aggregate structures also increased. In Figure 4.7.a, the absence of an aggregate

structure in the microscope supports that the formation of nanoparticles is sufficient within 2 hours in nanoscale. Additionally, it is clear that there is more aggregate structure in the images of nanoparticles after washings (Figure 4.7.b, d, f). In order to prevent this situation, the sonication time was increased to 15 min while suspending.

4.1.7. Small Volume

Since the enzyme will be loaded into HSA nanoparticles, the smaller volume of HSA nanoparticles production has been experienced. In experiment 8, a new synthesis was carried out with 10 mg of HSA. Nanoparticles were crosslinked for 2, 3, 4 hours with 0.2% w/w and 2.2% w/w genipin. The samples were suspended in ultrapure water and stored at 4°C. SEM images were taken with samples crosslinked with 0.2% w/w and 2.2% w/w genipin for 2, 3, 4 hours.

4.2. Characterization of Empty HSA Nanoparticles

Nanoparticles were characterized by examining FT-IR results, SEM images and Zeta-sizer results.

4.2.1. SEM Analysis

The morphological analysis of nanoparticles under the conditions in experiment 8 was carried out by SEM at 20 kV energy. The effect of crosslinking conditions of genipin like concentration and time on nanoparticle formation and morphology was investigated. SEM images of nanoparticles displayed according to crosslinking times (2h, 3h, 4h) and crosslinking concentrations (0.2% and 2.2% w/w genipin) are shown in Figure 4.8 and Figure 4.9. Empty HSA nanoparticles were observed to be spherical. As seen in the SEM images, it was also seen that uniform and small nanoparticles were synthesized for all types of nanoparticles. The size of nanoparticles crosslinked 2.2% w/w genipin concentration ranges from 12 to 32 nm (Figure 4.8). The size of nanoparticles crosslinked 0.2% w/w genipin concentration ranges from 11 to 23 (Figure 4.9). As the concentration increased, the size of nanoparticles increased as well. Additionally, when we compare the SEM images of Figure 4.8 and Figure 4.9, it is clearly seen that the crosslinked nanoparticles with high genipin concentration form aggregate structures within themselves.

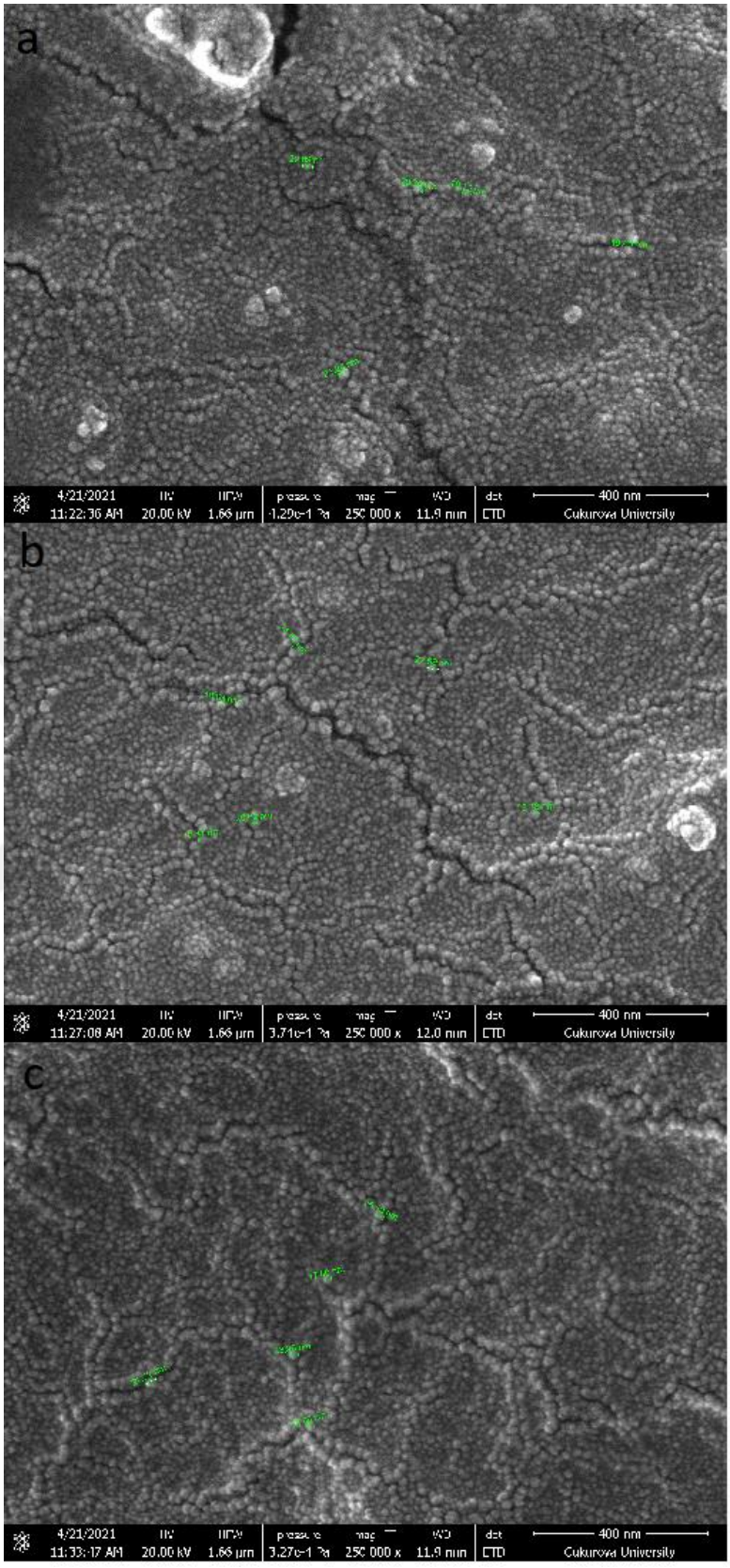

Figure 4.8. 2.2% w/w genipin a) Crosslinked for 2 hours b) Crosslinked for 3 hours c) Crosslinked for 4 hour

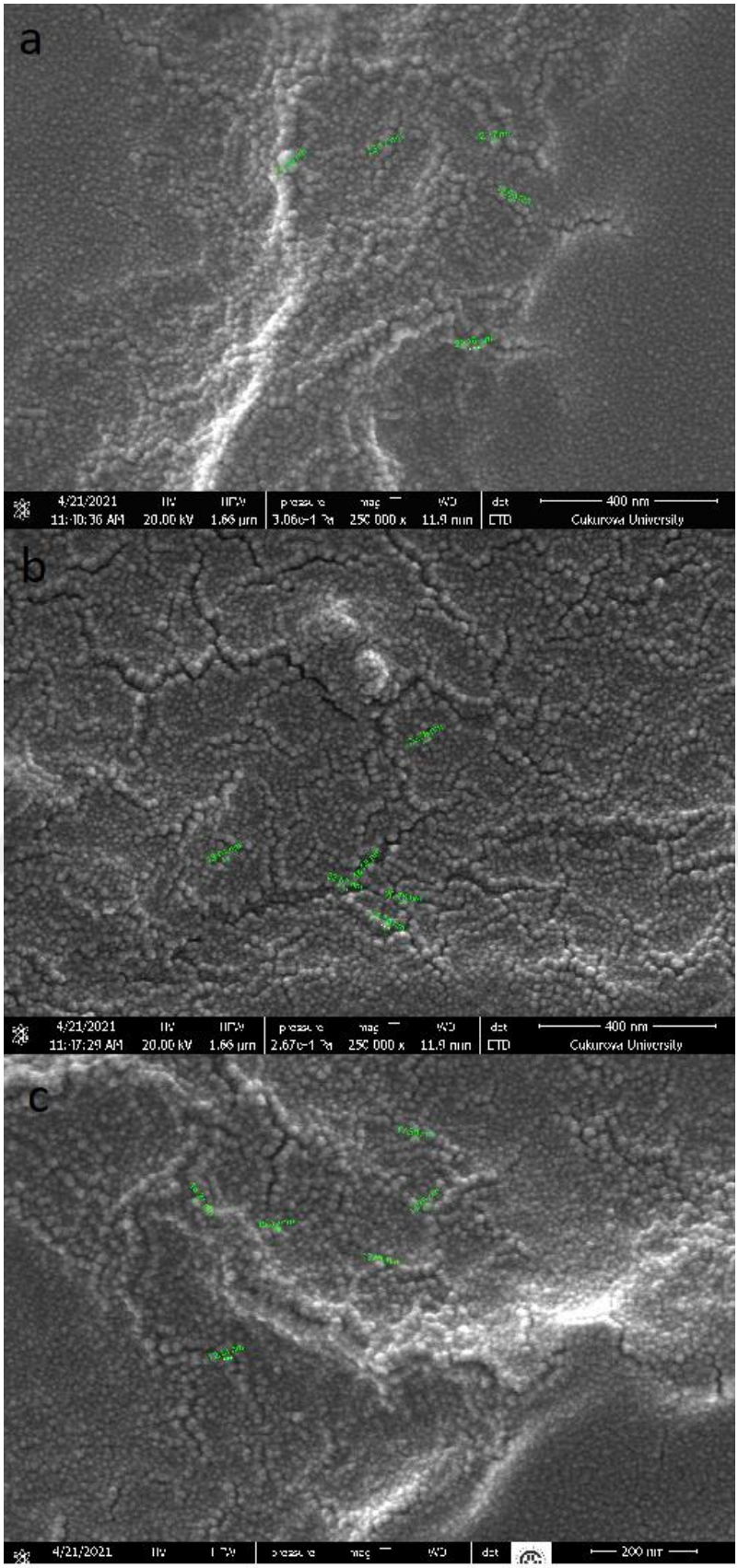

Figure 4.9. 0.2% w/w genipin a) Crosslinked for 2 hours b) Crosslinked for 3 hours c) Crosslinked for 4 hours.

To compare the change in particle size and their distribution, the diameter of nanoparticles was measured by ImageJ software and histogram graphs have been created (Figure 4.10 and Figure 4.11).

The average size of nanoparticles crosslinked with high genipin concentration for 2h, 3h, 4h was determined 20.475, 20.452, 22.398 respectively. It is observed that the size increases as the crosslinking time increases.

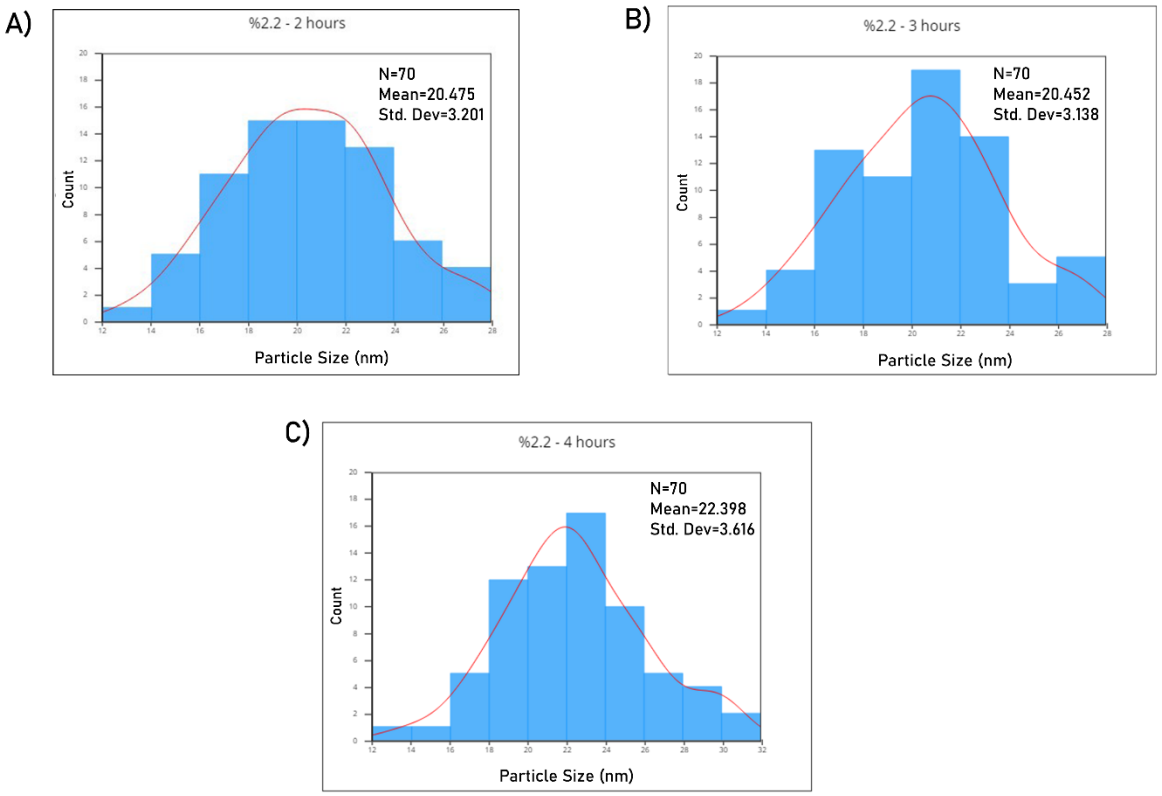

Figure 4.10. Size distribution of HSA nanoparticles crosslinked with 2.2% w/w gnp a) for 2 hours b)3 hours c) 4 hours.

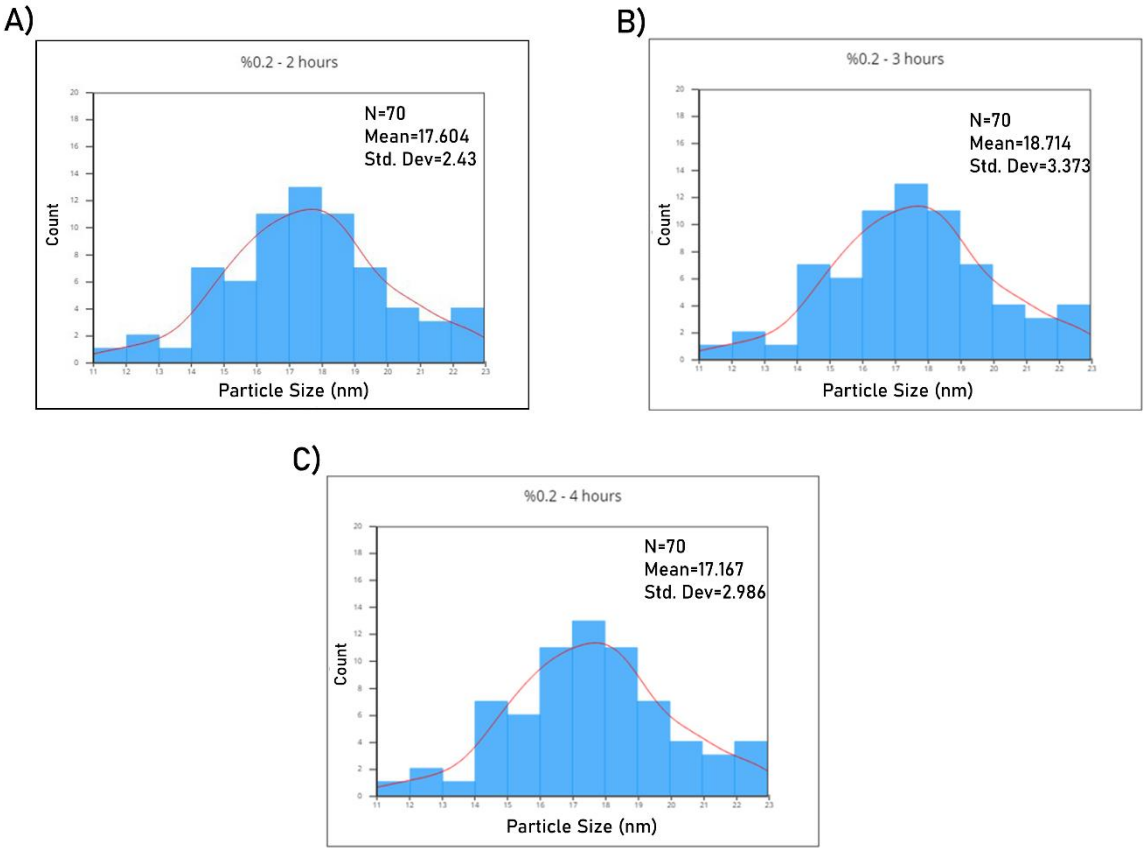

Figure 4.11. Size distribution of HSA nanoparticles crosslinked with 0.2% w/w gnp a) for 2 hours b) 3 hours c) 4 hours.

When we look at the size distribution histogram of nanoparticles crosslinked by low genipin concentration. The average size of nanoparticles crosslinked with low genipin concentration for 2h, 3h, 4h was determined 17.604, 18.714, 17.167 respectively. It is clearly observed that there is no significant difference (Figure 4.11). However, as the crosslinking time increases, the aggreagate structure slightly is observed (Figure 4.9)

Nanoparticles are taken up into the cell by various endocytosis pathways and nanoparticles up to 200 nm are simultaneously taken into the cell by multiple endocytotic pathways (Lee et al., 2014).

In the literature, the size of nanoparticles crosslinked with glutaraldehyde is ranging from 150-300 nm (Elzoghby et al., 2012; Langer et al., 2003). When compared with our study, crosslinking with genipin resulted in a significant decrease in nanoparticle size.

4.2.2. Size Distribution and Zeta-Potential Analysis Results

Zeta-potential and size distribution analysis of nanoparticles synthesized under the conditions in experiment 8 was performed by Zetasizer. The polydispersity index (PDI) expressing the particle size distribution and zeta-potentials expressing the surface charge were measured as well.

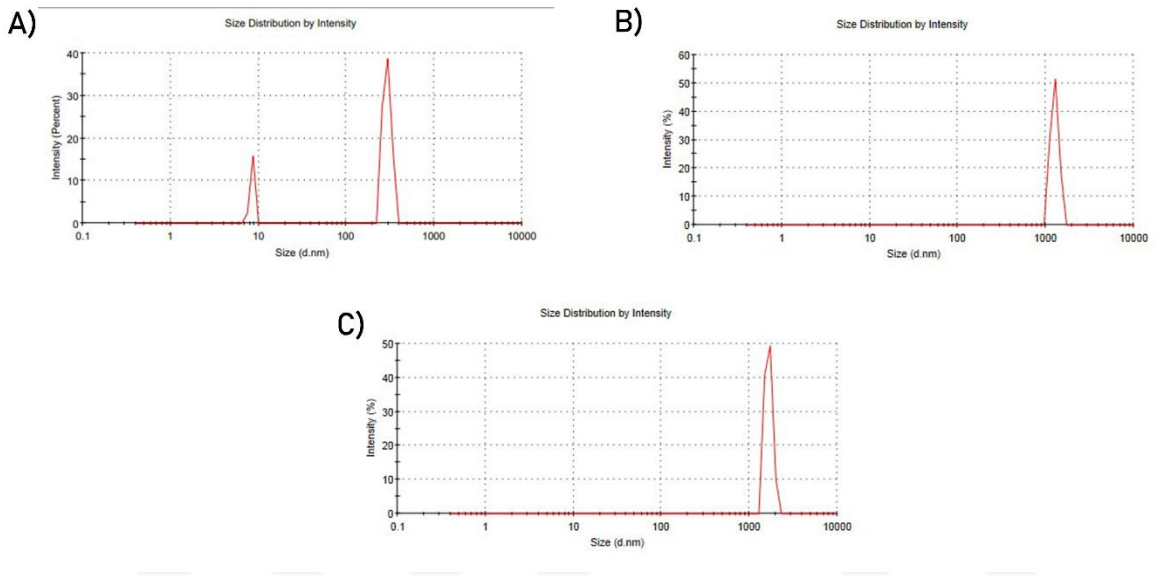

Figure 4.12. Size distribution of HSA nanoparticles crosslinked with 0.2% w/w gnp a) for 2 hours b) 3 hours c) 4 hours.

Size distribution graphs of nanoparticles crosslinked with 0.2% are shown in Figure 4.12 and the zeta-potential distribution graph is shown in Figure 4.13. The size distribution graph does not match the nanoparticle distribution graph drawn by Image J (Figure 4.11). This situation shows that nanoparticles tend to aggregate in an aqueous solution.

Other results of analysis are shown in Table 4.1. Zeta potential is a measure of repulsion between nanoparticles. Zeta potential results also show that stability of nanoparticles in suspension decreased, as genipin concentration increased.

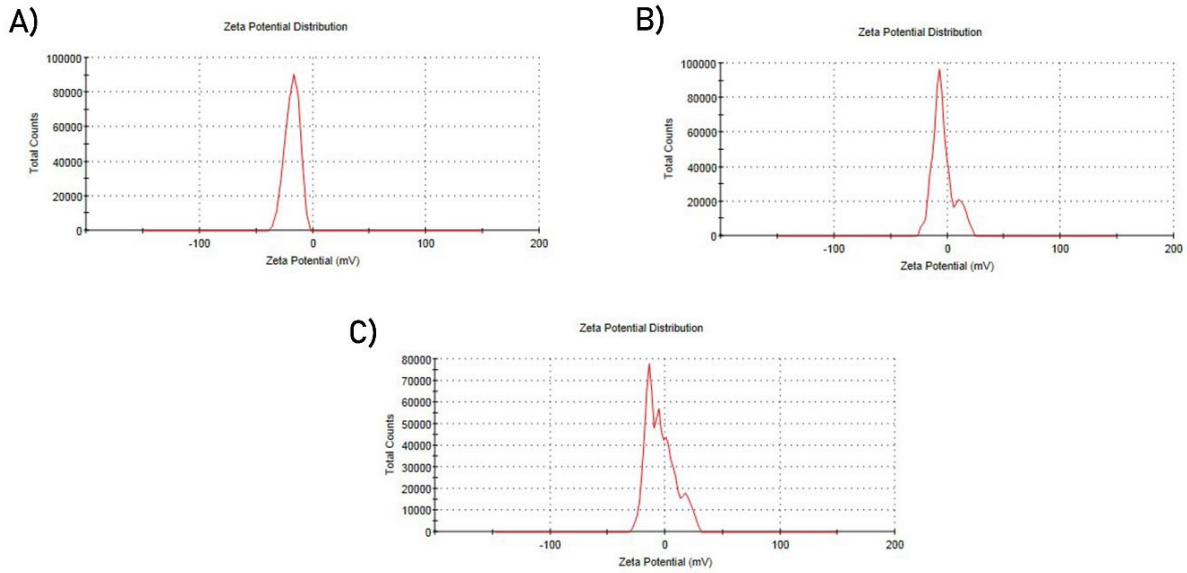

Figure 4.13. Zeta-potential of HSA nanoparticles crosslinked with 0.2% w/w gnp a) for 2 hours b) 3 hours c) 4 hours.

Table 4.1. Size, PdI and Z-pot results

	Z-ave (d.nm)	**PdI**	**Z-pot (mV)**
0.2% Gnp - 2 hours	323,5	0,668	-18.2
0.2% Gnp – 3 hours	3012	0,120	-4.05
0.2% Gnp – 4 hours	3884	1,000	-3.93

Size distribution graphs of nanoparticles crosslinked with 2.2% are shown in Figure 4.14 and the zeta-potential distribution graph is shown in Figure 4.15. The size distribution graph does not match the nanoparticle distribution graph drawn by Image J (Figure 4.10). This situation shows that nanoparticles tend to aggregate in an aqueous solution.

Other results of the analysis are shown in Table 4.2. Zeta potential results also show that the stability of nanoparticles in suspension decreased, as genipin concentration increased. A stable graph was not seen in the zeta-potential results (Figure 4.15).

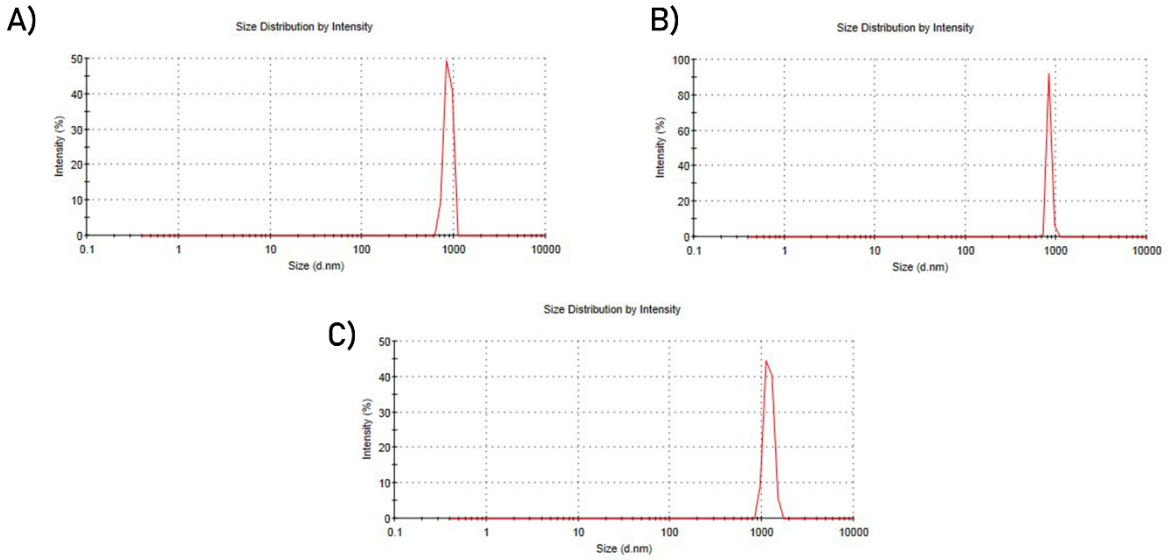

Figure 4.14. Size distribution of HSA nanoparticles crosslinked with 2.2% w/w gnp a) for 2 hours b) 3 hours c) 4 hours

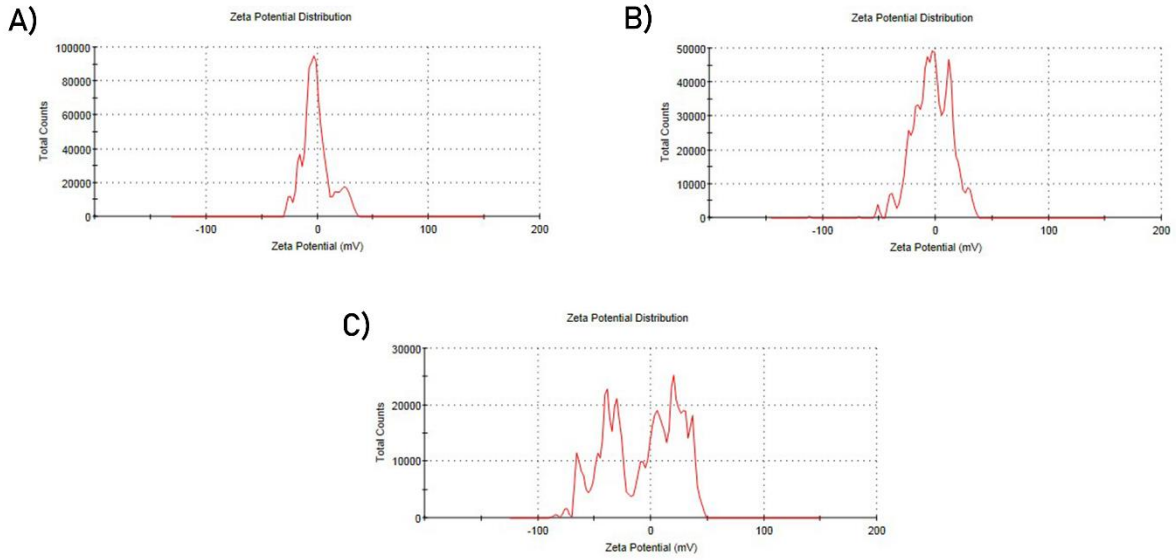

Figure 4.15. Zeta-potential of HSA nanoparticles crosslinked with 2.2% w/w gnp a) for 2 hours b) 3 hours c) 4 hours.

Table 4.2. Size, PdI and Z-pot results

	Z-ave (d.nm)	**PdI**	**Z-pot (mV)**
2.2% Gnp – 2 hours	1700	0.396	-1.21
2.2% Gnp – 3 hours	2666	0.552	-3.25
2.2% Gnp – 4 hours	2392	1000	-7.46

The ideal formulation of nanoparticles has the smallest size and the highest value of zeta potential, and the lowest polydispersity (Tarhini et al., 2020). Therefore, when the datas obtained were compared, the optimum condition of production was determined as crosslinked with 0.2% genipin for 2h. Additionally, this optimum condition was examined in different pH environments. The results are shown in Figure 4.16 and Table 4.3. It was observed that as the pH increase, the large aggregates decrease. pH has a significant effect on the size of nanoparticles and PdI. Z-average was decreased from 323,5 to 50,72 by increasing the pH from 7 to 9. PdI also was decreased from 0,668 to 0,227.

HSA is a negatively charged protein that has isoelectric pH of 4.7. Carboxyl and amino groups are protonated below the isoelectric point of the protein, resulting in a net positive charge. Conversely, above the isoelectric point they are not protonated and the net charge is negative. As for the size and PdI reduction, a similar impact of ionic strength increase could be applied to the pH variation. These differences in charges can alter protein electrostatic repulsion and trigger aggregation, which results in larger nanoparticles. This finding reveals that it is possible to modify the colloidal characteristics of HSA nanoparticles by varying the experimental parameters (Tarhini et al., 2020).

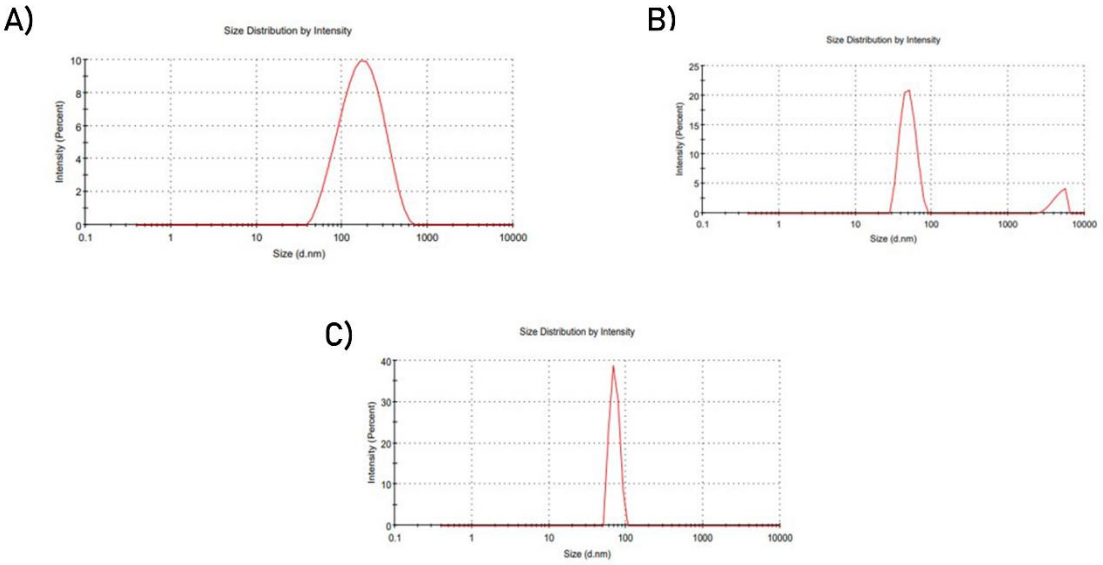

Figure 4.16. Size distribution of HSA nanoparticles crosslinked with 0.2% w/w genipin for 2 hours a) PBS b) pH=8 c) pH=9

Table 4.3. Z-ave and PdI results

	pH	**Z-ave (d.nm)**	**PdI**
0.2% Gnp – 2 hours	PBS (7.4)	144,6	0,278
0.2% Gnp – 2 hours	8	56,14	0,473
0.2% Gnp – 2 hours	9	50,72	0,227

4.2.3. FTIR Analysis Result

FTIR spectroscopy was used for the molecular analysis of nanoparticles crosslinked with 0.2% genipin for 2h. The result is shown in the Figure 4.17.

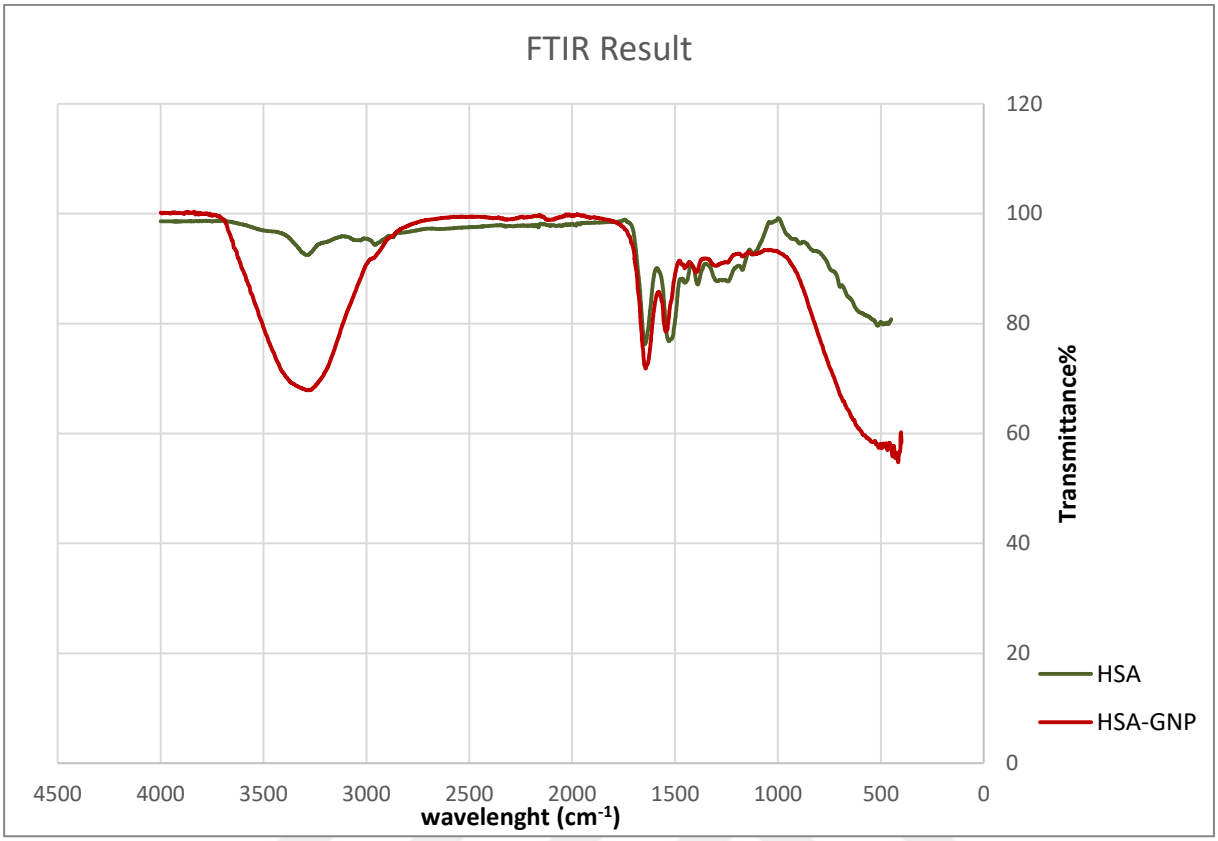

Figure 4.17. FTIR graph of non-crosslinked and genipin-crosslinked HSA nanoparticles

The range between 1670- 1620 cm^{-1} indicates an unsaturation bond. The specific peak is 1650 cm^{-1} for double bond carbon, or olefinic compounds (C=C). Interaction with other double bounds like C=C, C=O or aromatic rings can decrease intensity severely or severe absorption bands (Nandiyanto, Oktiani, & Ragadhita, 2019).

The characteristic peak at 3430 cm^{-1} reflects the stretching vibration of O-H groups. In the graph, there are two absorption peaks that correspond to amide groups: amide I (1600-1700 cm^{-1}) and amide II (1500-1600 cm^{-1}). Amide I mainly is appeared because of C=O stretching, otherwise, the amide II mainly indicates C-N stretching coupled with N-H bending (Ghosh et al., 2016; Nasir et al., 2017).

The spectrum of non-crosslinked HSA and genipin-crosslinked HSA nanoparticles is very similar to each other. The non-crosslinked HSA shows amide I peak at 1659 and when it is crosslinked with genipin, the small shift of the amide I was observed from 1659 to 1642 slightly. According to of shift in peak position, it can be said that the conformation of HSA has been

influenced by the genipin molecule (Daniel-Da-Silva, Salgueiro, & Trindade, 2013; Nasir et al., 2017).

4.3. Encapsulation of KLK6 into HSA Nanoparticles

4.3.1. The Effect of HSA Concentration

In experiment 9, neurosin encapsulation was carried out into where 10 mg of HSA, selected as the optimum condition, was crosslinked with 0.2% w/w genipin. 10 mg HSA and 10 µg neurosin were mixed in 500 µl ultrapure water for 15 minutes and 2 ml ethanol was added. Their images were taken by SEM (Figure 4.20). However, calculation of encapsulation efficiency and release studies could not be done, since Finetest KLK6 Human Elisa kit did not work with neurosin produced from E.coli. So, experiments were continued to work with neurosin expressed from the same cell as Elisa kit.

In experiment 10, nanoparticles were synthesized with new neurosin obtained from Finetest. Neurosin encapsulation was carried out into nanoparticles where 10 mg of HSA, selected as the optimum condition, was crosslinked with 0.2% w/w genipin. 10 mg HSA and 10 µg neurosin were mixed in 500 µl ultrapure water for 15 minutes and 2 ml ethanol was added. However, the collapse was observed after the addition of ethanol and sticking was seen on the beaker edges (Figure 4.18.b). However, the coagulation and sticking were removed by sonication. Then, crosslinking and washing processes are applied to nanoparticles.

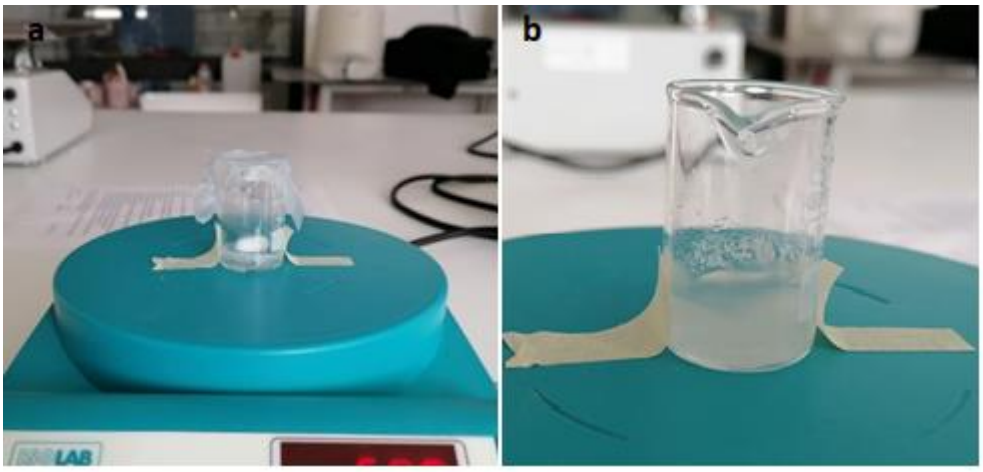

Figure 4.18. Exp 9, a) Mixing of neurosin and HSA before ethanol addition b) After ethanol addition

In experiment 11, by reducing the HSA concentration, 1 mg of HSA and 10 µg neurosin were mixed in 500 µl ultrapure water for 15 minutes and 2 ml of ethanol was added. In this study, slight coagulation was observed at the beaker. This coagulation was removed by sonication. It was allowed to crosslink with 0.2% w/w genipin for 2 hours.

4.3.2. Washing and Centrifuge Conditions

In experiments 9, 10 and 11, It was observed that 10 µg neurosin loaded HSA nanoparticles did not precipitate efficiently with ultrapure water and at 20.000 rpm, 4°C, 15 min, which was determined as an optimum condition to remove supernatant. Therefore, it was determined that the loaded nanoparticles should be precipitated in ultrapure water with 40% v/v ethanol as a wash solution by utilizing the precipitation effect of ethanol. At the same time, it was determined as 23.000 rpm, 4°C, 15 min for ultracentrifuge condition. The small nanoparticles were precipitated by increasing the centrifuge speed.

4.3.3. Encapsulation Efficiency of Neurosin

For experiments 9 and 10, encapsulation efficiency could not be calculated. In experiment 11, the encapsulation efficiency of neurosin loaded HSA nanoparticles was found as %99.9. The encapsulation efficiency of the loaded HSA nanoparticles was calculated according to equation 3.2 in section 3.2.9. The total amount of neurosin is the amount of neurosin mixed with HSA during synthesis. The amount of free neurosin is the amount of neurosin in the supernatant remaining in the upper phase after centrifugation. The amount of neurosin in the supernatant was calculated by the calibration curve.

Table 4.4. Result of neurosin encapsulation efficiency

Total Neurosin amount (ng)	**Free Neurosin amount (ng)**	**Mass of NP (mg)**	**Encapsulation efficiency (%)**
5,000	1,04	0,5	99,9

4.3.4. Characterization of Neurosin Loaded HSA Nanoparticles

The loaded nanoparticles were characterized by examining the SEM image. Size and zeta potential analyzes of neurosin loaded HSA nanoparitcles were performed using a zeta-sizer device.

4.3.4.1. Size Distribution and Zeta-Potential Analysis Results of Neurosin Loaded HSA Nanoparticles

In experiment 11, the zeta-sizer results of neurosin loaded nanoparticles were examined in different pH environments. The results are shown in Figure 4.19 and Table 4.6. It is observed that as the pH increase, the large aggregates decrease. However, compared to the empty nanoparticles, the adhesion property to each other increase even more. The loading of the enzyme caused the aggregation of the nanoparticles.

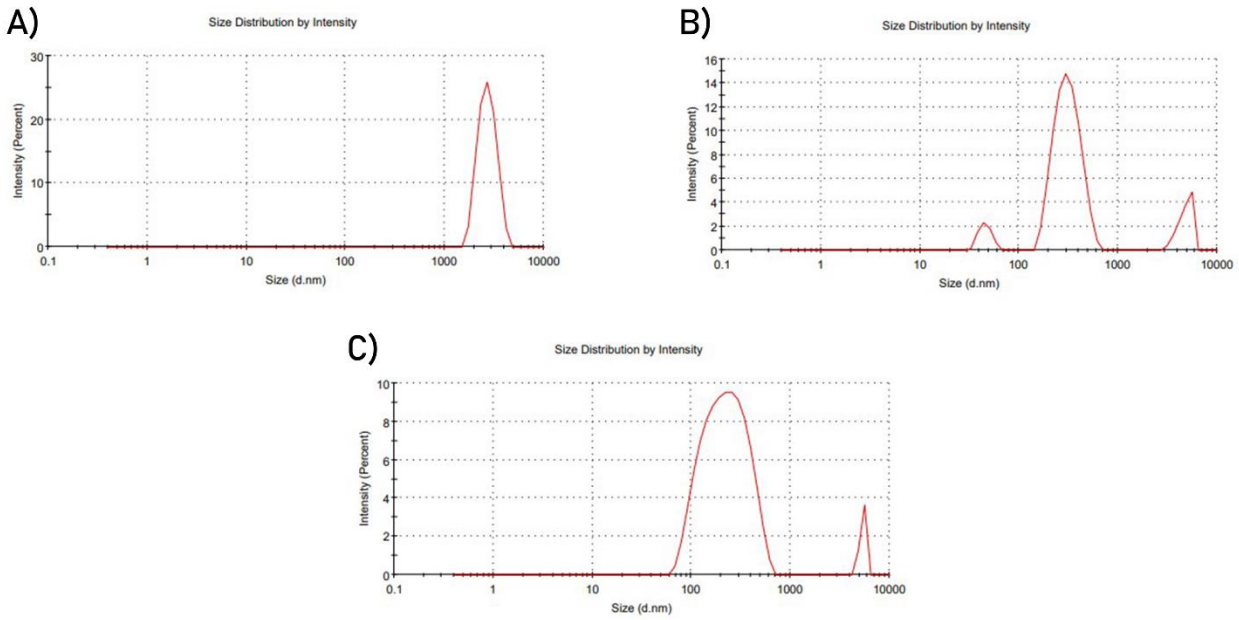

Figure 4.19. Exp 11, Size distribution of neurosin loaded nanoparticles a) pH=8 b) pH=9 c) PBS

Table 4.5. Experiment 11, Z-ave and PdI results

	pH	**Z-ave (d.nm)**	**PdI**
Neurosin-loaded Nanoparticles	8	301,1	0,609
Neurosin-loaded Nanoparticles	9	211,6	0,613
Neurosin-loaded Nanoparticles	PBS (7.4)	2763	0,419

4.3.4.2. SEM Images

The morphological analysis of neurosin loaded nanoparticles was carried out by SEM at 20 kV energy. Because of its small size, a clear image could not be taken in the SEM analysis. For experiment 9 where the synthesize was done with Raybiotech branded neurosin, it has been observed that the nanoparticles were small and homogeneous (Figure 4.20.a). When we look at the zoomed image, the size of nanoparticles was seen in the range of 8-12 nm (Figure 4.10.b).

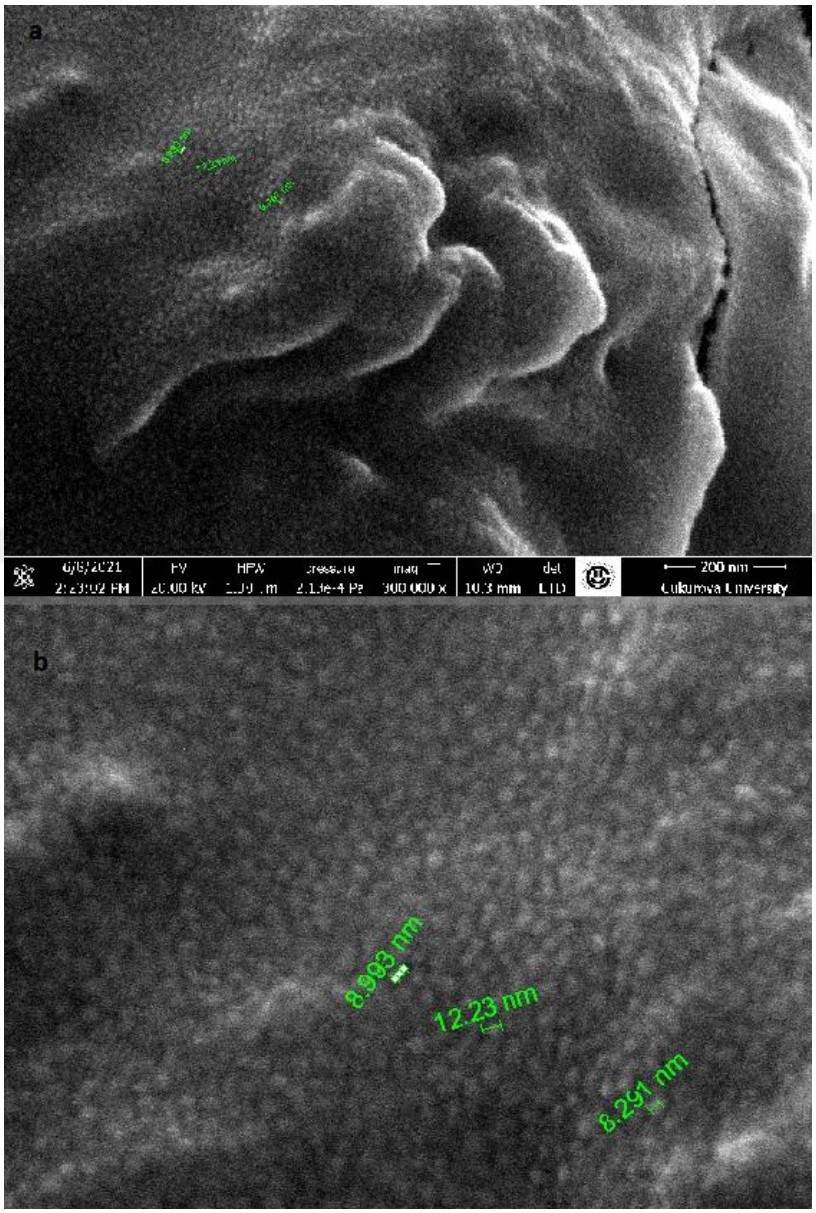

Figure 4.20. Exp 9**,** a) Sem images of neurosin loaded nanoparticles b) Zoomed sem images of neurosin loaded nanoparticles

For experiment 11 where the synthesize was done with Finetest branded neurosin, the size of nanoparticles appears smaller than 15 nm (Figure 4.21.a). The images of neurosin loaded HSA nanoparticles were found to be consistent with both brands (Figure 4.20.a, 4.21.a).

Additionally, when we examined the SEM images of experiment 11, it is clearly seen that the crystal structure of sugar was also found in the SEM images (Figure 4.21.b). Theralose sugar is included in the formulation of lyophilized neurosin used.

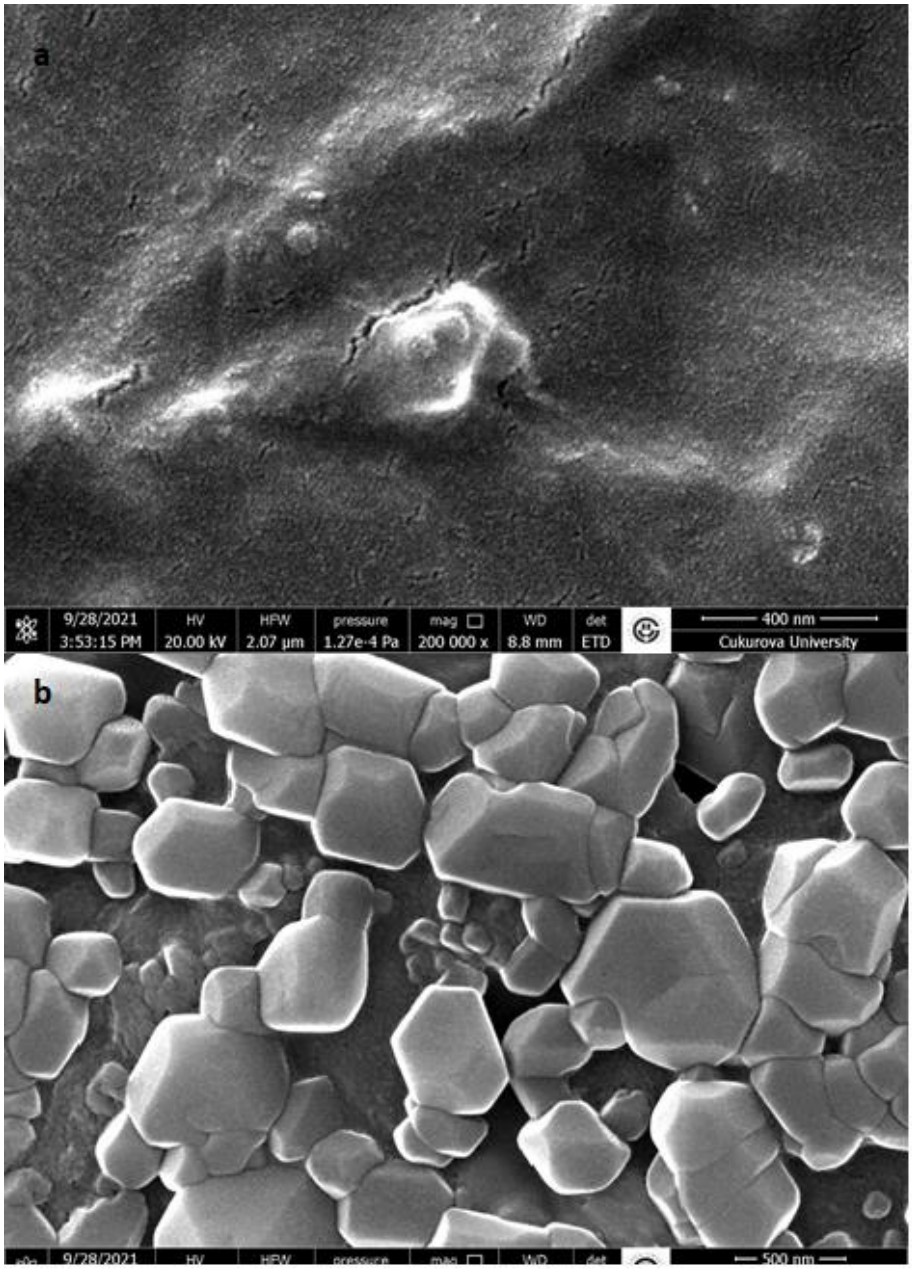

Figure 4.21. Exp 11, Sem images of neurosin loaded nanoparticles a) Nanoparticles b) Sugar

4.3.5. Neurosin Calibration Curve

The calibration curve created by absorbance values of neurosin solutions at different concentrations (Table 3.3) prepared as described in Section 3.2.8, using UV-Vis spectrophotometer at 450 nm wavelength, is given in Figure 4.22.

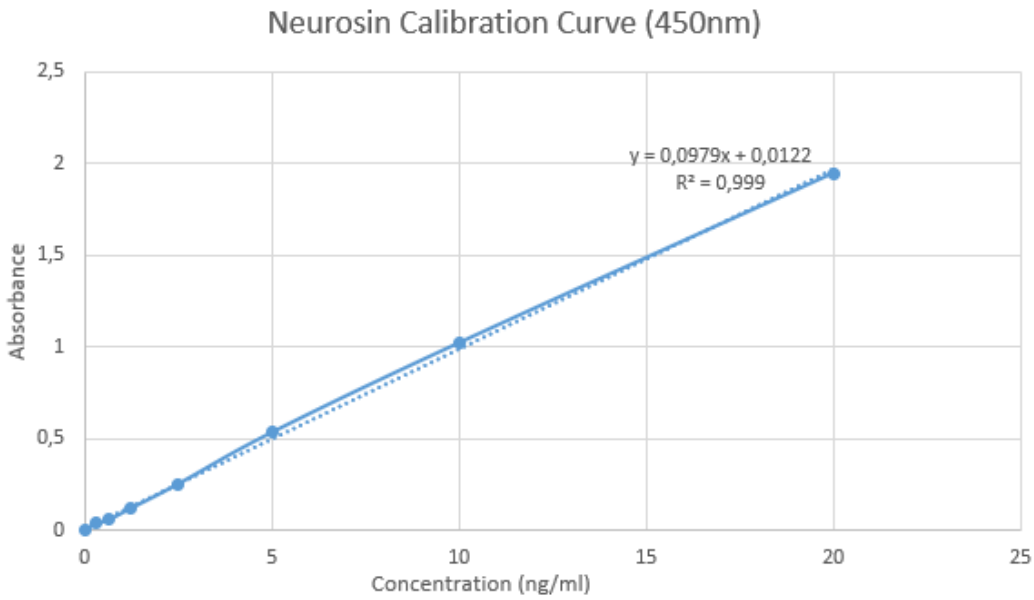

Figure 4.22. Neurosin calibration curve

For the encapsulation efficiency and release calculations, the calibration curve equation is created to determine the amount of neurosin was used.

4.3.6. *In vitro* Release Studies of Neurosin Loaded HSA Nanoparticles

Release studies of neurosin-loaded HSA nanoparticles were carried out inside a dialysis membrane in a shaking incubator. The release study with 500 ng HSA nanoparticles containing Neurosin was continued for 7 days. Samples taken at a certain times were calculated by UV measurements, the neurosin concentration in the release medium was calculated using the equation of calibration curve. Then, the amount of neurosin in ng was calculated cumulatively using the time-dependent amount calculation equation given in (3.1).

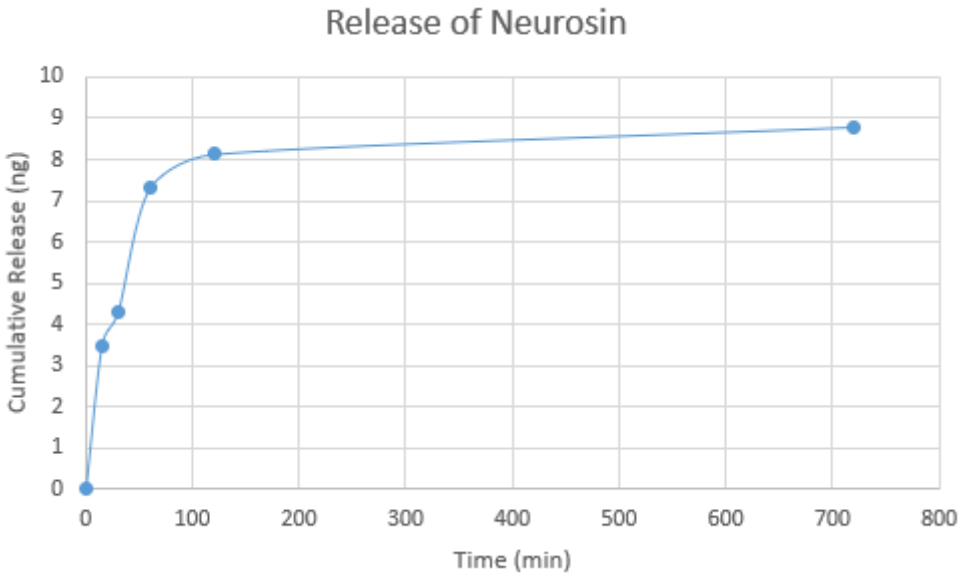

Figure 4.23. Release graph of neurosin

The cumulative release graph of HSA nanoparticles containing 10 µg neurosin is given in Figure 4.23. When the graph is examined, it was observed that neurosin was released with the burst effect in the first 30 minutes. Afterwards, it has been shown according to the samples taken for 7 days that drug release continues slowly. In the literature, burst effect is observed in the first 30 minutes in the release studies of nanoparticles in which BSA is crosslinked by genipin. The release system is similar to data from previous studies (Shahgholian, Rajabzadeh, & Malaekeh-Nikouei, 2017). However, the encapsulation efficiency and the data obtained in the release studies are not consistent with each other. While the efficiency of encapsulation was very high, the amount of data taken from the release was very low. It is observed that the reason is that the sugar in the formulation of neurosin causes sticking in the beaker and among themselves.

5. CONCLUSIONS

It has been proven by various studies in the literature that the neurosin enzyme inhibits the alpha-synuclein aggregate structure in Parkinson's patients.

In this thesis, optimization studies were carried out for HSA nanoparticles cross-linked with genipin, which is a natural crosslinker, instead of HSA nanoparticles cross-linked with glutaraldehyde, which has a toxic effect in the literature. In addition, it was aimed to encapsulate the neurosin enzyme into HSA nanoparticles cross-linked with genipin and to examine the controlled release of the molecule from the synthesized nanoparticle system. The general results of this thesis study are as follows:

In the first stage of the experiments, the synthesis was done by desolvation technique using 100 mg/ml, 50 mg/ml, 20 mg/ml HSA solutions to decide protein concentration. After adding ethanol to 100 mg/ml HSA concentration, coagulation was observed and nanoparticles could not be obtained. 50 mg/ml and 20 mg/ml concentrations were considered to be appropriate, and 20 mg/ml was used for small-scale studies.

In the crosslinking step, BSA nanoparticles were crosslinked with genipin for 24 hours at room temperature in the literature. Based on this study, HSA nanoparticles were left for crosslinking at room temperature for 24 hours. However, nanoparticles could not be produced. It was preferred to continue the studies with an incubator set at 37°C.

The activity of genipin accelerates by the increase in temperature. Considering the results of the analysis of the samples crosslinked for 2, 3, 4 hours, it was seen that 2 hours is an optimum time. As the hour increased, coagulation began to be observed.

In crosslinking performed with 500 and 600 rpm at magnetic stirrers, it was observed that working with 600 rpm reduced coagulation and a homogeneous distribution was obtained.

In studies with 2.2% and 0.2% w/w genipin concentrations, it was observed that genipin at high concentrations causes polymerization in itself and causes coagulation of nanoparticles. Low concentration was preferred.

The nanoparticles obtained by crosslinking 20 mg/ml HSA 0.2% w/w genipin at 37°C for 2 hours were chosen as the optimum condition. After synthesis, the average size of the nanoparticles was determined as 17,604 nm. Small and homogeneous nanoparticles were obtained. The zeta potential value was analyzed as -18.2 mV. The fact that it is not above 25 mV indicates that it is not fully stable.

In loading of neurosin studies, it was observed that the solution completely precipitated and adhered to the sides of the beaker after the addition of ethanol in the study with 20 mg/ml HSA. The HSA concentration was reduced to 2 mg/ml.

It was observed that the loading of 2 mg/ml HSA and 10 µg neurosin did not completely collapse due to the small size obtained in the centrifugation step. Washing procedures were continued with 40% ethanol. Ultracentrifuge speed was increased and continued with 23,000 rpm.

The encapsulation efficiency of neurosin-loaded HSA nanoparticles was calculated to be 99.9%. However, considering the neurosin encapsulation efficiency as 99.9%, there is an inconsistency between the encapsulation efficiency and the analysis of the release studies. As a source of this, the adhesion of HSA and neurosin to the glass beaker because of the addition of ethanol during nanoparticle synthesis prevented the HSA-neurosin interaction. However, it is clearly seen that the crystal structure of sugar was also found in the SEM analysis. Sugar is included in the formulation of lyophilized neurosin used. So, this situation is considering as the reason for sticking.

It was observed that the neurosin was released with the burst effect in the first 30 minutes and progressed steadily in the other days.

6. RECOMMENDATIONS

In the light of all these findings, it is thought that genipin cross-linked HSA nanoparticles, which are not included in the literature, can be used as a controlled release system. The absence of any nanoparticle studies with neurosin enzyme in the literature suggests that this study may serve as a model for neurosin.

The stability level of the genipin cross-linked nanoparticles synthesized in this thesis can be increased with various modifications for the release system. In addition, it may be recommended to examine the effect of neurosin-loaded nanoparticles on alpha-synuclein aggregates and to apply toxicity tests.

REFERENCES

Ashby, E. L., Kehoe, P. G., & Love, S. (2010). Kallikrein-related peptidase 6 in Alzheimer's disease and vascular dementia. *Brain Research*. doi:10.1016/j.brainres.2010.09.017

Bernett, M. J., Blaber, S. I., Scarisbrick, I. A., Dhanarajan, P., Thompson, S. M., & Blaber, M. (2002). Crystal structure and biochemical characterization of human kallikrein 6 reveals that a trypsin-like kallikrein is expressed in the central nervous system. *Journal of Biological Chemistry*. doi:10.1074/jbc.M202392200

Bi, L., Cao, Z., Hu, Y., Song, Y., Yu, L., Yang, B., … Han, Y. (2011). Effects of different cross-linking conditions on the properties of genipin-cross-linked chitosan/collagen scaffolds for cartilage tissue engineering. *Journal of Materials Science: Materials in Medicine*, *22*(1), 51–62. doi:10.1007/s10856-010-4177-3

Braak, H., Del Tredici, K., Rüb, U., De Vos, R. A. I., Jansen Steur, E. N. H., & Braak, E. (2003). Staging of brain pathology related to sporadic Parkinson's disease. *Neurobiology of Aging*. doi:10.1016/S0197-4580(02)00065-9

Christine, C. W., Starr, P. A., Larson, P. S., Eberling, J. L., Jagust, W. J., Hawkins, R. A., … Aminoff, M. J. (2009). Safety and tolerability of putaminal AADC gene therapy for Parkinson disease. *Neurology*, *73*(20), 1662–1669. doi:10.1212/WNL.0b013e3181c29356

Daniel-Da-Silva, A. L., Salgueiro, A. M., & Trindade, T. (2013). Effects of Au nanoparticles on thermoresponsive genipin-crosslinked gelatin hydrogels. *Gold Bulletin*, *46*(1), 25–33. doi:10.1007/s13404-012-0078-1

Dash, S., Murthy, P. N., Nath, L., & Chowdhury, P. (2010). Kinetic modeling on drug release from controlled drug delivery systems. *Acta Poloniae Pharmaceutica - Drug Research*, *67*(3), 217–223.

Dauer, W., & Przedborski, S. (2003). Parkinson ' s Disease : Mechanisms and Models, *39*, 889–909.

de Lau, L. M., & Breteler, M. M. (2006). Epidemiology of Parkinson disease. *Lancet Neurology*.

Defer, G. L., Geny, C., Ricolfi, F., Fenelon, G., Monfort, J. C., Remy, P., … Nguyen, J. P. (1996). Long-term outcome of unilaterally transplanted parkinsonian patients I. Clinical approach. *Brain*, *119*(1), 41–50. doi:10.1093/brain/119.1.41

Dong, J., Cui, Y., Li, S., & Le, W. (2016). Current Pharmaceutical Treatments and Alternative Therapies of Parkinson's Disease. *Current Neuropharmacology*, *14*(4), 339–

355. doi:10.2174/1570159x14666151120123025

Dreis, S., Rothweiler, F., Michaelis, M., Cinatl, J., Kreuter, J., & Langer, K. (2007). Preparation, characterisation and maintenance of drug efficacy of doxorubicin-loaded human serum albumin (HSA) nanoparticles. *International Journal of Pharmaceutics*. doi:10.1016/j.ijpharm.2007.03.036

Elsadek, B., & Kratz, F. (2012). Impact of albumin on drug delivery - New applications on the horizon. *Journal of Controlled Release*. doi:10.1016/j.jconrel.2011.09.069

Elzoghby, A. O., Samy, W. M., & Elgindy, N. A. (2012). Albumin-based nanoparticles as potential controlled release drug delivery systems. *Journal of Controlled Release*. doi:10.1016/j.jconrel.2011.07.031

Fan, Y., Winanto, & Ng, S. Y. (2020). Replacing what's lost: A new era of stem cell therapy for Parkinson's disease. *Translational Neurodegeneration*, *9*(1), 1–10. doi:10.1186/s40035-019-0180-x

Fanali, G., Di Masi, A., Trezza, V., Marino, M., Fasano, M., & Ascenzi, P. (2012). Human serum albumin: From bench to bedside. *Molecular Aspects of Medicine*. doi:10.1016/j.mam.2011.12.002

Feany, M. B., & Bender, W. W. (2000). A Drosophila model of Parkinson's disease. *Nature*. doi:10.1038/35006074

Fitzgerald, E., Murphy, S., & Martinson, H. A. (2019). Alpha-synuclein pathology and the role of the microbiota in Parkinson's disease. *Frontiers in Neuroscience*, *13*(APR), 1–13. doi:10.3389/fnins.2019.00369

Fu, M. H., Li, C. L., Lin, H. L., Chen, P. C., Calkins, M. J., Chang, Y. F., … Yang, S. H. (2015). Stem cell transplantation therapy in Parkinson's disease. *SpringerPlus*, *4*(1), 1–8. doi:10.1186/s40064-015-1400-1

Galisteo-González, F., & Molina-bolívar, J. A. (2014). Systematic study on the preparation of BSA nanoparticles. *Colloids and Surfaces B: Biointerfaces*. doi:10.1016/j.colsurfb.2014.09.028

Geibl, F. F., Henrich, M. T., & Oertel, W. H. (2019). Mesencephalic and extramesencephalic dopaminergic systems in Parkinson's disease. *Journal of Neural Transmission*, *126*(4), 377–396. doi:10.1007/s00702-019-01970-9

Ghosh, P., Singha Roy, A., Chaudhury, S., Jana, S. K., Chaudhury, K., & Dasgupta, S. (2016). Preparation of albumin based nanoparticles for delivery of fisetin and evaluation of its cytotoxic activity. *International Journal of Biological Macromolecules*, *86*, 408–

417. doi:10.1016/j.ijbiomac.2016.01.082

Gómez-Benito, M., Granado, N., García-Sanz, P., Michel, A., Dumoulin, M., & Moratalla, R. (2020). Modeling Parkinson's Disease With the Alpha-Synuclein Protein. *Frontiers in Pharmacology*, *11*(April), 1–15. doi:10.3389/fphar.2020.00356

Harris, J. P., Burrell, J. C., Struzyna, L. A., Chen, H. I., Serruya, M. D., Wolf, J. A., … Cullen, D. K. (2020). Emerging regenerative medicine and tissue engineering strategies for Parkinson's disease. *Npj Parkinson's Disease*, *6*(1). doi:10.1038/s41531-019-0105-5

Huang, X., & Brazel, C. S. (2001). On the importance and mechanisms of burst release in matrix-controlled drug delivery systems. *Journal of Controlled Release*, *73*(2–3), 121–136. doi:10.1016/S0168-3659(01)00248-6

Iwata, A., Maruyama, M., Akagi, T., Hashikawa, T., Kanazawa, I., Tsuji, S., & Nukina, N. (2003). Alpha-synuclein degradation by serine protease neurosin: Implication for pathogenesis of synucleinopathies. *Human Molecular Genetics*. doi:10.1093/hmg/ddg283

Kalia, L. V., & Lang, A. E. (2015). Parkinson's disease. *The Lancet*, *386*(9996), 896–912. doi:10.1016/S0140-6736(14)61393-3

Kasai, T., Tokuda, T., Yamaguchi, N., Watanabe, Y., Kametani, F., Nakagawa, M., & Mizuno, T. (2008). Cleavage of normal and pathological forms of α-synuclein by neurosin in vitro. *Neuroscience Letters*. doi:10.1016/j.neulet.2008.02.057

Klein, C., & Westenberger, A. (2012). Genetics of Parkinson's Disease Christine. *Cold Spring Harbor Perspectives in Medicine*. doi:10.1016/j.jconrel.2014.05.021

Kratz, F. (2008). Albumin as a drug carrier: Design of prodrugs, drug conjugates and nanoparticles. *Journal of Controlled Release*. doi:10.1016/j.jconrel.2008.05.010

Kratz, F. (2014). A clinical update of using albumin as a drug vehicle - A commentary. *Journal of Controlled Release*. doi:10.1016/j.jconrel.2014.03.013

Langer, K., Anhorn, M. G., Steinhauser, I., Dreis, S., Celebi, D., Schrickel, N., … Vogel, V. (2008). Human serum albumin (HSA) nanoparticles: Reproducibility of preparation process and kinetics of enzymatic degradation. *International Journal of Pharmaceutics*, *347*(1–2), 109–117. doi:10.1016/j.ijpharm.2007.06.028

Langer, K., Balthasar, S., Vogel, V., Dinauer, N., Briesen, H. Von, & Schubert, D. (2003). Optimization of the preparation process for human serum albumin (HSA) nanoparticles, *257*, 169–180. doi:10.1016/S0378-5173(03)00134-0

Lashuel, H. A., Overk, C. R., Oueslati, A., & Masliah, E. (2013). The many faces of α-

synuclein: From structure and toxicity to therapeutic target. *Nature Reviews Neuroscience*. doi:10.1038/nrn3406

Lee, H. J., Park, H. H., Kim, J. A., Park, J. H., Ryu, J., Choi, J., … Park, T. H. (2014). Enzyme delivery using the 30Kc19 protein and human serum albumin nanoparticles. *Biomaterials*, *35*(5), 1696–1704. doi:10.1016/j.biomaterials.2013.11.001

LeWitt, P. A., Rezai, A. R., Leehey, M. A., Ojemann, S. G., Flaherty, A. W., Eskandar, E. N., … Feigin, A. (2011). AAV2-GAD gene therapy for advanced Parkinson's disease: A double-blind, sham-surgery controlled, randomised trial. *The Lancet Neurology*, *10*(4), 309–319. doi:10.1016/S1474-4422(11)70039-4

Li, Y., Li, L., & Hölscher, C. (2016). Therapeutic Potential of Genipin in Central Neurodegenerative Diseases. *CNS Drugs*, *30*(10), 889–897. doi:10.1007/s40263-016-0369-9

Luo, R., Lin, M., Zhang, C., Shi, J., Zhang, S., Chen, Q., … Gao, F. (2020). Genipin-crosslinked human serum albumin coating using a tannic acid layer for enhanced oral administration of curcumin in the treatment of ulcerative colitis. *Food Chemistry*. doi:10.1016/j.foodchem.2020.127241

Magklara, A., Mellati, A. A., Wasney, G. A., Little, S. P., Sotiropoulou, G., Becker, G. W., & Diamandis, E. P. (2003). Characterization of the enzymatic activity of human kallikrein 6: Autoactivation, substrate specificity, and regulation by inhibitors. *Biochemical and Biophysical Research Communications*. doi:10.1016/S0006-291X(03)01271-3

Manickam, B., Sreedharan, R., & Elumalai, M. (2014). 'Genipin' – The Natural Water Soluble Cross-linking Agent and Its Importance in the Modified Drug Delivery Systems: An Overview. *Current Drug Delivery*, *11*(1), 139–145. doi:10.2174/15672018113106660059

Marks, W. J., Ostrem, J. L., Verhagen, L., Starr, P. A., Larson, P. S., Bakay, R. A., … Bartus, R. T. (2008). Safety and tolerability of intraputaminal delivery of CERE-120 (adeno-associated virus serotype 2-neurturin) to patients with idiopathic Parkinson's disease: an open-label, phase I trial. *The Lancet Neurology*, *7*(5), 400–408. doi:10.1016/S1474-4422(08)70065-6

Mathematical models of drug release. (2015). *Strategies to Modify the Drug Release from Pharmaceutical Systems*, 63–86. doi:10.1016/b978-0-08-100092-2.00005-9

Matrices, S. (1963). Mechanism of Sustained- Action Medication.

Menéndez-González, M., Padilla-Zambrano, H. S., Tomás-Zapico, C., & Fernández García,

B. (2018). Clearing extracellular alpha-synuclein from cerebrospinal fluid: A new therapeutic strategy in parkinson's disease. *Brain Sciences*, *8*(4), 6–11. doi:10.3390/brainsci8040052

Mi, F., Shyu, S., Peng, C., (2005). Characterization of ring-opening polymerization of genipin and pH-dependent cross-linking reactions between chitosan and genipin. *Journal of Polymer Science, Part A: Polymer Chemistry, (2005), 1985-2000, 43(10)*

Murakami, H., Kobayashi, M., Takeuchi, H., & Kawashima, Y. (2000). Further application of a modified spontaneous emulsification solvent diffusion method to various types of PLGA and PLA polymers for preparation of nanoparticles. *Powder Technology*. doi:10.1016/S0032-5910(99)00182-5

Nandiyanto, A. B. D., Oktiani, R., & Ragadhita, R. (2019). How to read and interpret ftir spectroscope of organic material. *Indonesian Journal of Science and Technology*, *4*(1), 97–118. doi:10.17509/ijost.v4i1.15806

Nasir, Z., Shakir, M. L., Wahab, R., Shoeb, M., Alam, P., Khan, R. H., & Mobin, M. (2017). Co-precipitation synthesis and characterization of Co doped SnO2 NPs, HSA interaction via various spectroscopic techniques and their antimicrobial and photocatalytic activities. *International Journal of Biological Macromolecules*, *94*, 554–565. doi:10.1016/j.ijbiomac.2016.10.057

Nouri, A., & Rafati, H. (2017). Preparation and characterization of paclitaxel-loaded Human Serum Albumin (HSA) nanoparticles using desolvation technique; Effect of manufacturing parameters on particle characteristics. *Journal of Bionanoscience*. doi:10.1166/jbns.2017.1446

Paarakh, M. P., Jose, P. A. N. I., Setty, C. M., & Peter, G. V. (2018). RELEASE KINETICS – CONCEPTS AND APPLICATIONS, 12–20.

Park, S. M., & Kim, K. S. (2013). Proteolytic clearance of extracellular α-synuclein as a new therapeutic approach against parkinson disease. *Prion*. doi:10.4161/pri.22850

Poewe, W., Seppi, K., Tanner, C. M., Halliday, G. M., Brundin, P., Volkmann, J., … Lang, A. E. (2017). Parkinson disease. *Nature Reviews Disease Primers*, *3*, 1–21. doi:10.1038/nrdp.2017.13

Radwan, S. E., El-kamel, A., Burgalassi, S., Zucchetti, E., & El-moslemany, R. M. (2021). Hyaluronic-Coated Albumin Nanoparticles for the Non-Invasive Delivery of Apatinib in Diabetic Retinopathy, (June).

Rahimnejad, M., Mokhtarian, N., & Ghasemi, M. (2009). Production of protein nanoparticles

for food and drug delivery system. *African Journal of Biotechnology*. doi:10.4314/ajb.v8i19.62445

Raza, C., Anjum, R., & Shakeel, N. ul A. (2019). Parkinson's disease: Mechanisms, translational models and management strategies. *Life Sciences*, *226*(March), 77–90. doi:10.1016/j.lfs.2019.03.057

Rizvi, S. A. A., & Saleh, A. M. (2018). Applications of nanoparticle systems in drug delivery technology. *Saudi Pharmaceutical Journal*, *26*(1), 64–70. doi:10.1016/j.jsps.2017.10.012

Sakho, E. H. M., Allahyari, E., Oluwafemi, O. S., Thomas, S., & Kalarikkal, N. (2017). *Dynamic Light Scattering (DLS). Thermal and Rheological Measurement Techniques for Nanomaterials Characterization* (Vol. 3). Elsevier Inc. doi:10.1016/B978-0-323-46139-9.00002-5

Sebak, S., Mirzaei, M., Malhotra, M., Kulamarva, A., & Prakash, S. (2010). Human serum albumin nanoparticles as an efficient noscapine drug delivery system for potential use in breast cancer: Preparation and in vitro analysis. *International Journal of Nanomedicine*. doi:10.2147/IJN.S10443

Shahgholian, N., Rajabzadeh, G., & Malaekeh-Nikouei, B. (2017). Preparation and evaluation of BSA-based hydrosol nanoparticles cross-linked with genipin for oral administration of poorly water-soluble curcumin. *International Journal of Biological Macromolecules*. doi:10.1016/j.ijbiomac.2017.06.083

Singh, R., & Lillard, J. W. (2009). Nanoparticle-based targeted drug delivery. *Experimental and Molecular Pathology*, *86*(3), 215–223. doi:10.1016/j.yexmp.2008.12.004

Singhvi, G., & Singh, M. (2011). REVIEW : IN-VITRO DRUG RELEASE CHARACTERIZATION MODELS, *II*(I).

Spencer, B., Michael, S., Shen, J., Kosberg, K., Rockenstein, E., Patrick, C., … Masliah, E. (2013). Lentivirus mediated delivery of neurosin promotes clearance of wild-type α-synuclein and reduces the pathology in an α-synuclein model of LBD. *Molecular Therapy*. doi:10.1038/mt.2012.66

Spencer, B., Valera, E., Rockenstein, E., Trejo-Morales, M., Adame, A., & Masliah, E. (2015). A brain-targeted, modified neurosin (kallikrein-6) reduces α-synuclein accumulation in a mouse model of multiple system atrophy. *Molecular Neurodegeneration*, *10*(1), 1–17. doi:10.1186/s13024-015-0043-6

Stoker, T. B., & Barker, R. A. (2020). Recent developments in the treatment of Parkinson's

Disease. *F1000Research*, *9*, 1–12. doi:10.12688/f1000research.25634.1

Stoker, T. B., Torsney, K. M., & Barker, R. A. (2018). Emerging treatment approaches for Parkinson's disease. *Frontiers in Neuroscience*, *12*(OCT), 1–10. doi:10.3389/fnins.2018.00693

Tarhini, M., Greige-Gerges, H., & Elaissari, A. (2017). Protein-based nanoparticles: From preparation to encapsulation of active molecules. *International Journal of Pharmaceutics*. doi:10.1016/j.ijpharm.2017.01.067

Tarhini, M., Pizzoccaro A, Benlyamani I et al. (2020). Nanoparticles as nanovector carriers for proteins: Application to the antibacterial proteins "neutrophil elastase" and "secretory leukocyte protease inhibitor". *International Journal of Pharmaceutics, 579.*

Terada, M., Suzuki, G., Nonaka, T., Kametani, F., Tamaoka, A., & Hasegawa, M. (2018). The effect of truncation on prion-like properties of -synuclein. *Journal of Biological Chemistry*. doi:10.1074/jbc.RA118.001862

Vargas, J. Y., Grudina, C., & Zurzolo, C. (2019). The prion-like spreading of α-synuclein: From in vitro to in vivo models of Parkinson's disease. *Ageing Research Reviews*, *50*(January), 89–101. doi:10.1016/j.arr.2019.01.012

Wang, S., Liu, S., Zhang, Y., He, J., Coy, D. H., & Sun, L. (2020). Human Serum Albumin (HSA) and Its Applications as a Drug Delivery Vehicle Abstract. *Health Science Journal*, *14*(2), 1–8. doi:10.36648/1791-809X.14.2.698

Wennström, M., Surova, Y., Hall, S., Nilsson, C., Minthon, L., Boström, F., … Nielsen, H. M. (2013). Low CSF Levels of Both α-Synuclein and the α-Synuclein Cleaving Enzyme Neurosin in Patients with Synucleinopathy. *PLoS ONE*, *8*(1). doi:10.1371/journal.pone.0053250

Wilczewska, A. Z., Niemirowicz, K., Markiewicz, K. H., & Car, H. (2012). Nanoparticles as drug delivery systems.

Wolf, M., Wirth, M., Pittner, F., & Gabor, F. (2003). *Stabilisation and determination of the biological activity of L-asparaginase in poly(D,L-lactide-co-glycolide) nanospheres*. In *International Journal of Pharmaceutics*. doi:10.1016/S0378-5173(03)00071-1

Zhao, S., Wang, W., Huang, Y., Fu, Y., & Cheng, Y. (2014). Paclitaxel loaded human serum albumin nanoparticles stabilized with intermolecular disulfide bonds. *MedChemComm*. doi:10.1039/c4md00200h

Zhou, G., Jin, X., Zhu, P., Yao, J., Zhang, Y., Teng, L., … Hong, W. (2016). Human serum albumin nanoparticles as a novel delivery system for cabazitaxel. *Anticancer Research*.